

AD-A164 045

DEVELOPMENT OF A FUEL SPILL/VAPOR MIGRATION MODELING
SYSTEM(U) TRACER TECHNOLOGIES ESCONDIDO CA*
N G ENGLAND ET AL. DEC 85 AFMRL-TR-85-2089

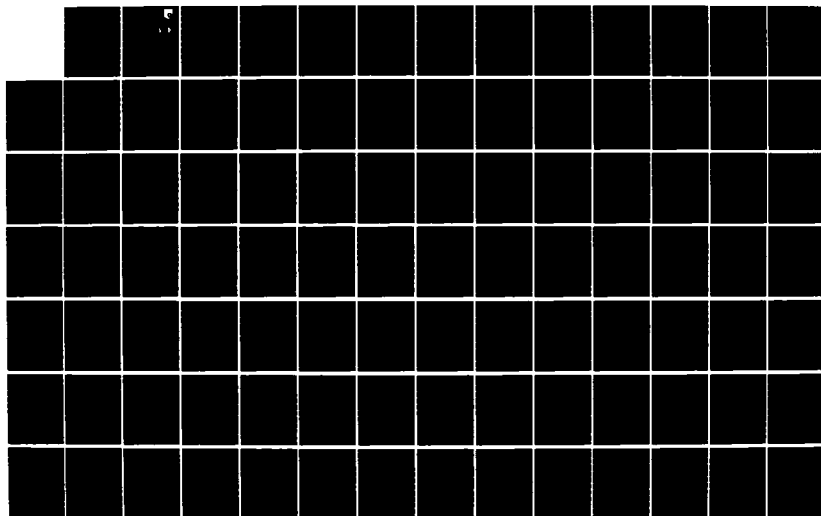
1/2

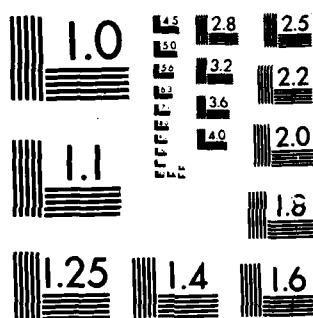
UNCLASSIFIED

F33615-83-C-2472

F/G 21/4

NL





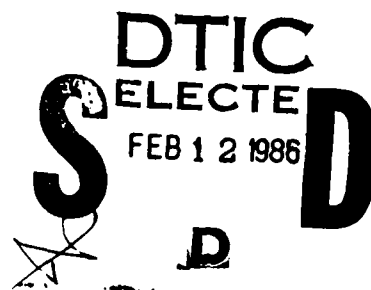
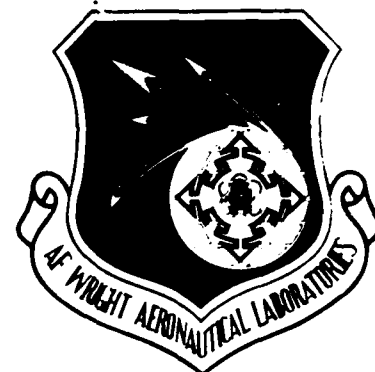
MICROCOPY RESOLUTION TEST CHART
NATIONAL BUREAU OF STANDARDS-1963-A

AFWAL-TR-85-2089

DEVELOPMENT OF A FUEL SPILL/VAPOR MIGRATION MODELING SYSTEM

W.G. England
L.H. Teuscher

TRACER TECHNOLOGIES
2120 WEST MISSION ROAD
ESCONDIDO, CALIFORNIA 92025



DECEMBER 1985

FINAL REPORT FOR PERIOD OCTOBER 1984 - MARCH 1985

APPROVED FOR PUBLIC RELEASE; DISTRIBUTION UNLIMITED.

AERO PROPULSION LABORATORY
AIR FORCE WRIGHT AERONAUTICAL LABORATORIES
AIR FORCE SYSTEMS COMMAND
WRIGHT-PATTERSON AIR FORCE BASE, OHIO 45433

86 2 11 004

AD-A164 045


DTIC FILE COPY


NOTICE

When Government drawings, specifications, or other data are used for any purpose other than in connection with a definitely related Government procurement operation, the United States Government thereby incurs no responsibility nor any obligation whatsoever; and the fact that the government may have formulated, furnished, or in any way supplied the said drawings, specifications, or other data, is not to be regarded by implication or otherwise as in any manner licensing the holder or any other person or corporation, or conveying any rights or permission to manufacture, use, or sell any patented invention that may in any way be related thereto.


This report has been reviewed by the Office of Public Affairs (ASD/PA) and is releasable to the National Technical Information Service (NTIS). At NTIS, it will be available to the general public, including foreign nationals.

This technical report has been reviewed and is approved for publication.


JON R. MANHEIM
Project Engineer
Fire Protection Branch
Fuels and Lubrication Division


ROBERT G. CLODFELTER, Chief
Fire Protection Branch
Fuels and Lubrication Division

FOR THE COMMANDER


ROBERT D. SHERRILL, Chief
Fuels and Lubrication Division
Aero Propulsion Laboratory

"If your address has changed, if you wish to be removed from our mailing list, or if the addressee is no longer employed by your organization please notify AFWAL/POSH, W-PAFB, OH 45433 to help us maintain a current mailing list".

Copies of this report should not be returned unless return is required by security considerations, contractual obligations, or notice on a specific document.

UNCLASSIFIED

SECURITY CLASSIFICATION OF THIS PAGE

AD-A164045

REPORT DOCUMENTATION PAGE

1a. REPORT SECURITY CLASSIFICATION UNCLASSIFIED			1b. RESTRICTIVE MARKINGS NONE	
2a. SECURITY CLASSIFICATION AUTHORITY N/A			3. DISTRIBUTION/AVAILABILITY OF REPORT APPROVED FOR PUBLIC RELEASE; DISTRIBUTION UNLIMITED	
2b. DECLASSIFICATION/DOWNGRADING SCHEDULE N/A				
4. PERFORMING ORGANIZATION REPORT NUMBER(S)			5. MONITORING ORGANIZATION REPORT NUMBER(S) AFWAL-TR-85-2089	
6a. NAME OF PERFORMING ORGANIZATION TRACER TECHNOLOGIES		6b. OFFICE SYMBOL (If applicable)	7a. NAME OF MONITORING ORGANIZATION AERO PROPULSION LABORATORY (AFWAL/POSH) AIR FORCE WRIGHT AERONAUTICAL LABORATORIES	
6c. ADDRESS (City, State and ZIP Code) ESCONDIDO CA 92025			7b. ADDRESS (City, State and ZIP Code) WRIGHT-PATTERSON AFB OH 45433-6563	
8a. NAME OF FUNDING/SPONSORING ORGANIZATION AERO PROPULSION LABORATORY		8b. OFFICE SYMBOL (If applicable) AFWAL/POSH	9. PROCUREMENT INSTRUMENT IDENTIFICATION NUMBER F33615-84-C-2472	
8c. ADDRESS (City, State and ZIP Code) WRIGHT-PATTERSON AFB OH 45433-6563			10. SOURCE OF FUNDING NOS.	
			PROGRAM ELEMENT NO. 65502F	PROJECT NO. 3005
			TASK NO. 20	WORK UNIT NO. 27
11. TITLE (Include Security Classification) DEVELOPMENT OF A FUEL SPILL/VAPOR MIGRATION MODELING SYSTEM				
12. PERSONAL AUTHOR(S) W. G. ENGLAND AND I. H. TEUSCHER				
13a. TYPE OF REPORT FINAL		13b. TIME COVERED FROM OCT 84 TO MAR 85	14. DATE OF REPORT (Yr., Mo., Day) December 1985	
			15. PAGE COUNT 106	
16. SUPPLEMENTARY NOTATION				
17. COSATI CODES			18. SUBJECT TERMS (Continue on reverse if necessary and identify by block number)	
FIELD	GROUP	SUB. GR.	VAPOR MIGRATION, FUEL SPILL	
21	04			
20	04			
19. ABSTRACT (Continue on reverse if necessary and identify by block number) The system of handling aircraft fuels and/or missile propellants can be subject to failure. Such system failures could result in a fuel/propellant spill and subsequently result in the release of potentially explosive or toxic vapors into the atmosphere. The results of the Phase I effort included a review of Air Force experience in aircraft fuel spills and the development of models to predict the vapor generation and migration of fuel spilled or sprayed into the atmosphere. These models were then applied to typical sizes of spills and estimates made of the hazard region around the spill. The results of the effort include an identification of the important parameters which influence the modeling results and estimates of the hazard region. The projected hazard region is somewhat smaller than present regulations require.				
20. DISTRIBUTION/AVAILABILITY OF ABSTRACT UNCLASSIFIED/UNLIMITED <input checked="" type="checkbox"/> SAME AS RPT. <input type="checkbox"/> DTIC USERS <input type="checkbox"/>			21. ABSTRACT SECURITY CLASSIFICATION UNCLASSIFIED	
22a. NAME OF RESPONSIBLE INDIVIDUAL JON R. MANHEIM			22b. TELEPHONE NUMBER (Include Area Code) (513) 255-6980	22c. OFFICE SYMBOL AFWAL/POSH

U.S. DEPARTMENT OF DEFENSE
SMALL BUSINESS INNOVATION RESEARCH PROGRAM
PHASE 1—FY 1984
PROJECT SUMMARY

Topic No. 109

Military Department/Agency USAF

Name and Address of Proposer

TRACER TECHNOLOGIES
2120 W. Mission Road, Suite M
Escondido, CA. 92025

Name and Title of Principal Investigator

Walter G. England, Ph.D. President, Chief Scientist

Proposer's Title

Development of a Fuel Spill/Vapor Migration Modeling System

Technical Abstract (Unclassified) (Limit To Two Hundred Words)

The system of handling aircraft fuels and/or missile propellants can be subject to failure. Such system failures could result in a fuel/propellant spill and subsequently result in the release of potentially explosive or toxic vapors into the atmosphere. The results of the Phase I effort included a review of Air Force experience in aircraft fuel spills and the development of models to predict the vapor generation and migration of fuel spilled or sprayed into the atmosphere. These models were then applied to typical sizes of spills and estimates made of the hazard region around the spill. The results of the effort include an identification of the important parameters which influence the modeling results and estimates of the hazard region. The projected hazard region is somewhat smaller than present regulations require.

Anticipated Benefits/Potential Commercial Applications of the Research or Development

Further development of the modeling system would benefit the U.S. Air Force by providing more accurate assessments for systems safety purposes. This could reduce unnecessary costs in ground operations and enable an increase in sortie generation rate. The developed system would be applicable to other military services as well as other fuels, such as missile fuels, and could be useful for system safety studies for commercial operators.

TABLE OF CONTENTS

1.0 Introduction	1
Program Objectives.	2
Summary of Results.	2
2.0 Technical Discussion	5
Source Model Requirements	6
Evaporation rate of JP-4	7
Liquid Pool Definition	11
Droplet Dynamics	11
Modeling Atmospheric Dispersion	13
Wind Conditions.	14
Atmospheric Stability.	14
Modeling	15
Axi-Symmetric Dispersion Model	18
Quasi-Three Dimensional Dispersion Model	21
Results	25
Literature Review.	25
Liquid Spill Model Results	27
Spray Model Results.	30
Dispersion Model Results	32
3.0 Conclusion and Recommendations	35

Appendix A	POOL
Appendix B	DROP
Appendix C	AXISYM
Appendix D	DISCO
Appendix E	Physical Properties
Appendix F	Sample Model Results



Accession For	
NTIS CRA&I	<input checked="" type="checkbox"/>
DTIC TAB	<input type="checkbox"/>
Unannounced	<input type="checkbox"/>
Justification	
By _____	
Distribution /	
Availability Codes	
Dist	Avail and/or Special
A-1	

LIST OF ILLUSTRATIONS

<u>Figure</u>		<u>Page</u>
2.1	Dynamics on JP4 Fuel Droplet	12
2.2	Temperature Profiles Indicating Lapse Rates: Slightly Unstable (C), Neutral (Dry Adiabatic), Neutral (D), and Slightly Stable (E)	16
2.3	POOL Vaporization Rate	28
A-1	Flowchart POOL Sources Model.. . . .	A-3
B-1	Flowchart DROPLET Source Model	B-3
C-1	Flowchart AXISYM dispersion Model	C-6
D-1	Flowchart DISCO Dispersion Model	D-10
D-2	Subroutine Input 1	D-12
D-3	Subroutine Setev	D-14
E-1	Drag Coefficient as a Function of Reynolds Number From (E2)	E-3
E-2	DrageCoefficient VS. Wind Speed as A Function of Droplet Diameter	E-5

LIST OF TABLES

<u>Table</u>		<u>Page</u>
2.1	Stability Classification by T/ Z	17
2.2	Summary Average Spill Frequency	26
2.3	Summary of Liquid Spill Results	29
E-1	Variations in	E-8
E-2	Turbulence Scale Lengths ()	E-8
E-3	Ratio of Horizontal and Vertical Diffusivities Versus Stability Class	E-9

1.0 INTRODUCTION

The loading and off-loading of fuel from aircraft is a process in which a significant system failure can occur. Such a failure could result in a release of flammable liquid and vapor. The migration of the potentially hazardous fuel vapors pose a threat to the safety of nearby personnel as well as to ground support equipment and other aircraft. When considering safety and economics of ground support operations, the accurate prediction of the physical behavior of the fuel releases is extremely important. While overly conservative and simplistic simulation models could be used to provide assessment of personnel safety and equipment vulnerability relative to the fires resulting from fuel vapors, these types of models can suggest mitigations that are unreasonable and which could seriously restrict ground support operations.

Tracer Technologies understands that the development of models which can accurately predict all possible accident events would be extremely expensive and unrealistic. Private industry has invested much time and money during the past decade toward the development of dispersion models/methodologies which can predict vapor migration/dispersion from various spills of flammable materials. Personnel at Tracer Technologies were responsible for the development of many of these models and calculational methods which have been successfully employed by the oil and gas industry. The purpose of this study was to modify and add to these models in order to derive a family of models which could be used routinely by the U.S. Air Force to study the potential consequences relative to leakages and spills of fuels. The models would then provide input to system safety engineering analysis and promote the development of cost effective and optimal material handling procedures for ground support operations.

PROGRAM OBJECTIVES

The technical objectives of the program as outlined in the original proposal to the Air Force were:

- 1 - Define the types and sizes of fuel spills expected at military ground support operations.
- 2 - Define the range of conditions under which the fuel spills occur at military bases and ground support operations.
- 3 - Develop or modify existing Tracer Technologies numerical models to define time dependent vapor source rates. These rates will be dependent upon fuel characteristics, storage and transfer methodologies, and environmental conditions.
- 4 - Execute the models in an analysis designed to aid in identifying the key physical parameters which govern the behavior of various types of spills envisioned.
- 5 - Modify and develop two dimensional dispersion models capable of providing realistic results for small to medium spills that can occur at Air Force ground support operations.

SUMMARY OF PROGRAM RESULTS

The five objectives noted have been completed with particular emphasis of JP4 fuel. This material is the most volatile of the fuels presently in use in military aircraft and presents the greatest hazard. This emphasis was agreed upon during initial technical meetings with Air Force experts. A review of the possible kinds of releases that could occur during typical refueling operations indicated that all of the releases could be fit into the general catagories of (1) vent spills or releases which occur during refueling as gaseous releases, (2) liquid pool spills which would occur if a fuel line failed and liquid

material was spilled on the ground, and (3) pressurized hose breaks which could result in the spraying of liquid droplets into the atmosphere. These types of scenerios were then considered as the generic kinds of spills which would be used in the model development portion of the contract.

An examination of the literature and discussions with personnal at both Norton AFB and Wright Patterson AFB have served to define probable spill types and sizes for this study. Ciccone and Graves (1), in a study to determine the methods for neutralization of DOD aircraft fuel spills, determined that spills could be catagorized as small, medium or large as follows; small: 0-4 gallons, medium: 5-42 gallons, and large: greater that 42 gallons. Discussions with present Air Force engineering personnel indicate that present operating procedures would allow failures of approximately this size given a specific scenerio. For example, a 3" diameter fueling hose 50 feet long (typical of that used) contains approximately 18.4 gallons. Allowing an operator a delay time of 1 to 5 seconds to respond to an emergency and cause system shut down, a total spill of 26 gallons to 56 gallons would occur. For purposes of the calculations performed during phase 1 of this study, two spill sizes were selected, 4 gallons and 40 gallons. The smaller spill was chosen since it represented the upper bound of the most probable spill grouping, while the larger spill represented the a median estimate between the "medium" and "large" spill categories.

The spill of fuel could be expected to occur outside or within ground shelters. In the former, all meteorological conditions must be taken into account. In the latter, low wind speed conditions will predominate. Therefore, during this study, two dispersion models, each representing one of these cases, was developed to accurately assess Air Force needs. Models were developed for the source characterization as well as for the transport and dilution of the resulting vapor clouds in the atmosphere. These models can be applied to specific situations

to evaluate the potential hazard area resulting from fuel spills.

The two source models developed were (1) a liquid pool spill model which includes time dependent heat and mass transfer effects, and (2) liquid droplet spray model which includes time dependent particle dynamics as well as heat and mass transfer effects. The transport and dispersion models include (1) a steady state dispersion model describing the diffusion of vapor from a steady source under moderate wind conditions and any atmospheric stability, and (2) a time dependent vapor dispersion model specifically for low speed wind conditions. The model theory is described in section 2.0 of this report while the actual codes are discussed in Appendices A through D. Appendix E contains a review of the parameters utilized in the model calculations presented and Appendix F provides sample outputs from the source models as well as the dispersion models.

The models were developed in such a manner that data input requirements can vary from very simple to complex. In the case of minimum initial data, only the spill scenario, the spill size, a wind speed at a specific height, and the atmospheric stability need be specified. Should it be available, complete atmospheric wind speed profiles, spray droplet size distributions, and source specifics such as fuel line pressure, hole size, etc. may be included in the calculations.

Tracer Technologies has proposed a phase II of the program which would consist of both continued development of the models, including the completion of a modified set of models which can be programmed on hand held calculators for field use, and an experimental program which will add significant credibility to the close in dispersion coefficients required to accurately assess fuel spills. These proposed future study requirements are outlined in detail in section 3.0 of this report.

2.0 TECHNICAL DISCUSSION

Modeling the failure of an aircraft fuel spill is done in two discrete steps. The first requires the determination of the source rate of flammable gases into the atmosphere. The second step is the prediction of the dispersion of the resulting flammable vapors. These two steps will yield the concentration of the fuel as functions of both time and position. One can then analyze the results to determine the extent of the safety hazard.

In order to calculate the source rate, Tracer Technologies has developed two models which account for tank or pressurized line spills. Pure vapor sources are directly input into the dispersion models. Since the primary hazard associated with JP4 fuel is a fire, the models need to deal only with minimum concentrations on the order of 1%. The lower flammability limit for JP4 is 1.3% (2). Should toxicity become a major concern with other types of fuels, much lower concentrations become important and changes to the developed models would be required.

The source models require a description of the physical parameters and conditions associated with the JP4 tank or fueling system. For tanks, geometric dimensions such as tank height, diameter, and any confinement devices such as dikes that may be in the immediate area are of importance. For fueling systems, the physical parameters are required as well as line pressures, temperatures, and delivery rates of the incoming fuel. Vent vapor flows require only the flow rate and exit area be described. For non-pressurized flows, the fuel will exit as a liquid and form a pool. For pressurized flows, the fluid may exit as a gas, a liquid, and thus predict time dependent vapor flow. Environmental conditions such as air fuel, and ground temperatures and wind speeds are also required. Should they not be specified, default values are built into the models. The vapor flow rate, given as a function of time, is input into one

of the two dispersion models developed. These models, developed for low or moderate wind speeds, require a description of the environmental conditions. Specifically, a wind speed and associated height and a description of the atmospheric stability is required. The models are capable of taking into account complete wind profiles should that information be available. The downwind dispersion of the incoming vapor source is calculated as a function of both time and position.

2.1 Source Model Requirements

The vapor source models require that the evaporation rate of JP4 fuel droplets or pools be described. The estimate involves a description of the total mass transfer process from the bulk of the liquid to the atmosphere, the heat transfer between the surrounding air, the ground, and the droplet or pool, and the loss/gain of energy from the liquid to the atmosphere through radiation processes. In addition to the evaporation terms, the dynamics of a droplet from a high pressure line leak must be described, as well as the size and thickness of any liquid pool forming. The description of the processes in this section are organized as follows: initially the heat and mass transfer processes are discussed since they are common to both models; secondly, the liquid pool model is be discussed; and finally, the vapor source associated with a break in a pressurized fuel spill is described. The physical parameters that describe JP4 are important to all of these calculations. JP4 fuel properties were obtained from reference (2), "Handbook of Aviation Fuel Properties". The data was compiled by the CRC Aviation Handbook Advisory Group from the latest known sources on each particular subject. Where conflicts arose owing to discrepancies in source material, they were resolved by decision of the Group. The data was published in 1983.

2.1.1 Evaporation Rates of JP4 Fuel

The problem considered is that of determining the rate of evaporation of JP4 as a function of temperature, wind speed, atmospheric conditions, solar radiation, the dimensions of the pool or droplet, and the volatility and diffusion characteristics of the fuel. The methodology is similar to that utilized by MacKay and Matsugu (3). This estimate requires a description of the total mass transfer process from the liquid to the atmosphere. The mass transfer process can include the liquid phase mass transfer resistance, which controls the rate of transfer of material from the liquid to the interface and depends on the diffusivities and the flow conditions in the liquid, and the transfer from the interface to the atmosphere. In this problem, only the transfer from the interface to the atmosphere is of importance since liquid concentration gradients are assumed to be insignificant. The vapor composition is assumed to equal that of the liquid and the liquid composition is assumed to remain constant with time. A vapor phase mass transfer coefficient is defined in equation (1) which gives the mass flux as a function of the vapor pressure driving force which is the difference between the JP4 vapor pressure at the surface P and the vapor pressure in the atmosphere P_{∞} .

$$(1) \quad N = K_m (P - P_{\infty}) / RT_{liq}$$

The value of P is not well known. Comparisons of the theory with droplet evaporation experiments (ref 4) were made and a value of P inferred which resulted in good agreement between the two. This procedure is described in more detail in Appendix E of this report.

K_m is a function of the transport conditions in the atmosphere immediately above the spill or surrounding the droplet.

2.1.1.1 Heat Transfer

An evaporating drop or liquid pool generally has a temperature close to that of the atmosphere and/or ground. At high rates of evaporation, JP4 may be considerably cooler due to evaporative enthalpy losses. It may warm, however, due to absorption of solar radiation, or heat conduction from the ground. To permit accurate predictions of evaporation rates, these effects must be quantified and the liquid temperature related to local conditions. The liquid temperature is determined by the direct heat transfer from the air, from the ground if considering a pool, the incident solar radiation, the emitted pool radiation, the rate of evaporation, the enthalpy of evaporation and the depth and temperature history of the pool or droplet. For the model developed here, the pool or droplet is considered to be of uniform temperature.

2.1.1.2 Velocity Characteristics of the Lower Atmosphere

The velocity profile above the JP4 pool and surrounding the droplets are critical in controlling the eddy diffusivity and the droplet drag. It was convenient to follow Sutton (5) and assume that the wind velocity profile follows a power law as indicated below in which U is the windspeed, U_1 is the windspeed at a specific height (1 meter) and Z is the height.

$$(2) \quad U = U_1 Z^{\frac{n}{2-n}}$$

The exponent n is a function of ground roughness and temperature profile in the atmosphere (stability). Typical values are from 0.25 to 1.00. For average atmospheric conditions a value of 0.25 for n is reasonable (5). Sutton has shown that using the Von Karman similarity principle and this assumed velocity profile,

the turbulent diffusivity can be expressed as a function of the velocity and the mass transfer coefficient can be deduced as equation 1 where C is a constant and X is the pool or droplet diameter. C is taken from experimental data.

$$(3) \quad K_m = CU^{0.78}X^{-0.11}$$

2.1.1.3 Theory

From the heat and mass transfer analogy (6), the heat and mass transfer coefficients can be related as follows:

$$(4) \quad (St_m) (Sc)^{0.67} = (St_h) (Pr)^{0.67}$$

thus

$$K_h = K_m \rho c_p (Sc/Pr)^{0.67}$$

The rate of heat transfer from the atmosphere is $K_h (T_A - T_{liq}) A$ cal/hr where T_A and T_{liq} are the atmospheric and liquid temperatures and A is the surface area. The heat transfer from the ground is similarly expressed as $K_c (T_G - T_{liq}) A$ where K_c is the heat transfer coefficient from the ground to the liquid, and T_G is the ground temperature.

For liquid pools, solar radiation is calculated as the incident direct solar radiation and scattered sky radiation (L), which reaches the earth's surface. A proportion of this is reflected, this being quantified by a surface albedo "a". The heat input from solar radiation will thus be $(1-a)LA$ cal/hr.

The loss by long wave radiation from the pool is $\epsilon_p \sigma T_{liq}^4 A$ where ϵ_p is the emissivity of the pool for long wavelength radiation and σ is the Stefan-Boltzmann constant. This term in the equation was only taken into account for liquid pool spills.

Evaporative cooling will cause a heat loss of

$$(5) K_m AW \Delta H^v \Delta P / RT$$

where W is the molecular weight of the JP4 fuel, ΔH^v the enthalpy of vaporization and ΔP the vapor pressure driving force.

Combining these heat flux terms with the mass transfer effects of evaporating JP4, the differential equation describing the temperature variation of the perfectly mixed pool with time can be written,

$$(6) \frac{dT_{liq}}{dt} = \frac{A}{mc_{ph}} \left\{ (1-a)L - \epsilon_p \sigma T_{liq}^4 + e_a \sigma T_a^4 + CU^q X^r (\rho_v C_{pv} (S_c/P_r)^{0.67} (T_a - T_{liq}) - W \Delta H^v \Delta P / RT_p) + K_c (T_g - T_{liq}) \right\}$$

The equation is integrated numerically to determine T_{liq} as a function of time. Once T_{liq} is known, the rate of evaporation

and cumulative mass losses are calculated using equation 3 and the mass conservation equation.

2.1.2 Liquid Pool Definition

The physical parameters which describe a liquid pool were determined using data from Ciccone and Graves (1). In their study of fuel tank leak classification, they measured the surface area of spills as a function of the overall spill size. An analysis of the data presented lead to the conclusion that the thickness of the liquid pool, for spill sizes considered in this study, would be approximately 0.0005 meters. This was treated as a constant in the pool source rate model with the pool area then calculated from the spill volume. Equation 5 was integrated and the temperature of the liquid was assumed constant through out.

2.1.3 Droplet Dynamics

JP4 fuel emitted from a broken or burst fueling line exits as liquid droplets. The dynamics of the droplets are necessary to describe the vapor source. Figure 2.1 shows the forces acting on the drop as it passes through the atmosphere. The equations describing the motion are

$$(7) \quad D_y - W = M_{liq} \frac{dv}{dt}, \quad D_x = M_{liq} \frac{dU}{dt}$$

where the drag force (assumed for a sphere) is expressed as

$$(8) \quad D = C_D \frac{1}{2} \rho a \bar{V}^2 A_s$$

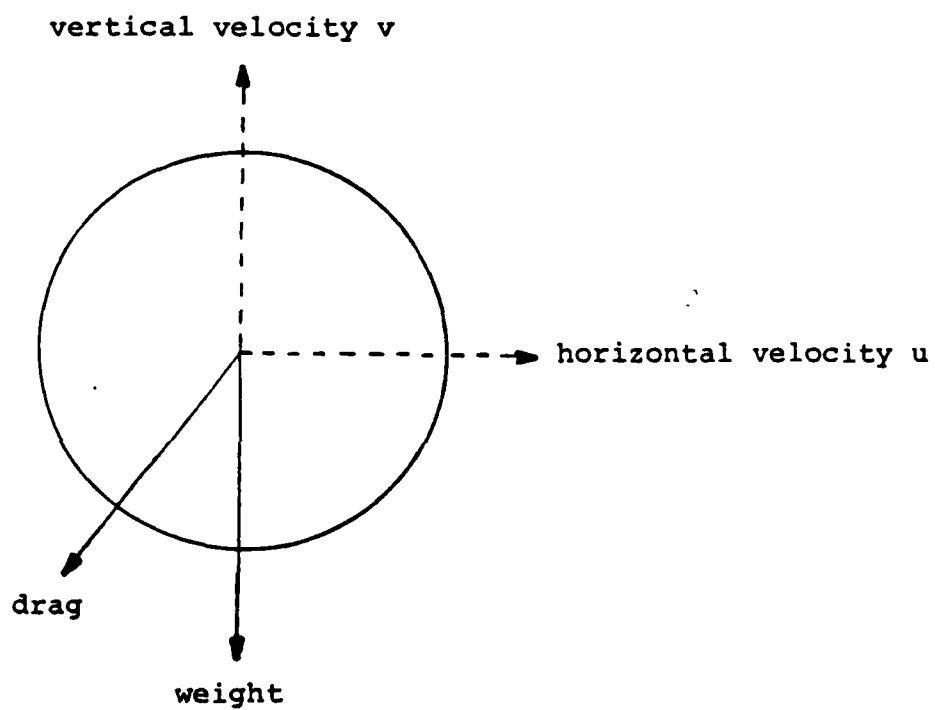


Figure 2-1
Dynamics on JP4 Fuel Droplet

and can be positive or negative, \bar{V} is the total velocity of the droplet, and A_s is the droplet frontal area. The weight is expressed as

$$(8) W = \rho_l \text{VOL}_{\text{drop}} g = \frac{4}{3} \pi r_{\text{drop}}^3 \rho_l g$$

The equations are integrated numerically for U and V, with the droplet evaporation accounted for using equations (1) and (6) to calculate a new droplet radius and mass evaporation.

2.2 Modeling Atmospheric Dispersion

With the source rate calculation complete, attention is turned to dispersion of the vapors. The ambient wind will begin to advect the vapor cloud downwind. Diffusional forces will act to disperse the vapors outward diluting the cloud and buoyancy forces, if present, will cause the cloud to rise or slump adding to the dispersion. All of these factors must be accounted for in order to accurately predict concentrations at locations away from the failure as functions of time.

Atmospheric diffusional forces are, as one would expect, strongly influenced by the local wind field and the stability of the atmosphere. The wind guides the direction of the cloud movement, and its strength influences the degree of air entrainment in the vapor cloud. The stability of the atmosphere is the tendency of buoyancy forces to enhance or oppose vertical motion. The atmospheric stability is a function of many factors, but one of the most important is surface or ground heating. Hence, the type

of surface; sand, asphalt, concrete, etc. and degree of cloud cover can be important parameters.

Wind Conditions

Wind speeds are the primary factor in determining the transport of the vapor cloud. One of the two major effects of the wind is to advect the cloud downwind moving the hazardous zone. Higher winds will move the cloud greater distances which can be a very negative factor from a safety standpoint. The higher winds can, however, have a beneficial effect in that higher winds generate higher turbulent levels in the atmosphere. The greater the turbulence, the greater the dispersion diluting the cloud down to safe concentration levels.

Specifying wind conditions can be a very difficult task. Wind speed and direction often change considerably from one hour to the next. The effect of these fluctuations is to spray the flammable material over a much wider area than would be predicted by specifying a single direction. This tends to make concentration predictions far downwind conservative due to the increased dilution.

Atmospheric Stability

More important than turbulent dispersion produced by eddies caused by the wind are those due to convection from density gradients. This convection dispersion is strongly influenced by surface heating and the vertical temperature distribution in the atmosphere. When air is heated from below, upward moving convective currents develop. These are caused since the lower air is hotter and hence more buoyant than the air above. When these buoyancy forces enhance the vertical mixing, the atmosphere is described as unstable. If the opposite occurs, the colder air tends to oppose vertical motion. In this situation the air is considered stable.

The stability of the atmosphere can be characterized by examining the rate at which the air temperature changes as one moves up in altitude. This rate of temperature change is known as the lapse rate. In dry air, if an air parcel is displaced vertically and is always in equilibrium with its surroundings (hence adiabatic), the lapse rate is approximately 1 C/100 m. Lapse rates less than this tend towards instability while those greater tend to be more stable. Figure 2.2 shows examples of these graphically. The stability of the atmosphere is generally broken into seven classes based on the lapse rate. These are specified by the letters A through G corresponding to extremely unstable to extremely stable. Table 2.1 shows this breakdown.

Modeling

The traditional method for modeling the dispersion of a substance in the atmosphere is to assume diffusion coefficients are independent of position and that the diffusion follows Fick's Law. By further assuming that the wind moves at an average speed, also independent of position, one arrives at the well-known gaussian equation. This predicts a binormal concentration distribution transverse to the wind as one moves downwind of the source. One predicts the diffusion coefficients based on the stability of the atmosphere.

This type of modeling is fairly good provided the source is neutrally buoyant and the other assumptions are met. However, when dealing with the type of releases that occur from pipeline breaks or tank failures this type of modeling is inappropriate. As discussed earlier, the wind field is not independent of position and is, in fact, a strong function of height near the ground. Also the vapor clouds are not always neutrally buoyant. In many cases, buoyant effects may dominate the atmospheric transport. For these reasons more sophisticated models are needed.

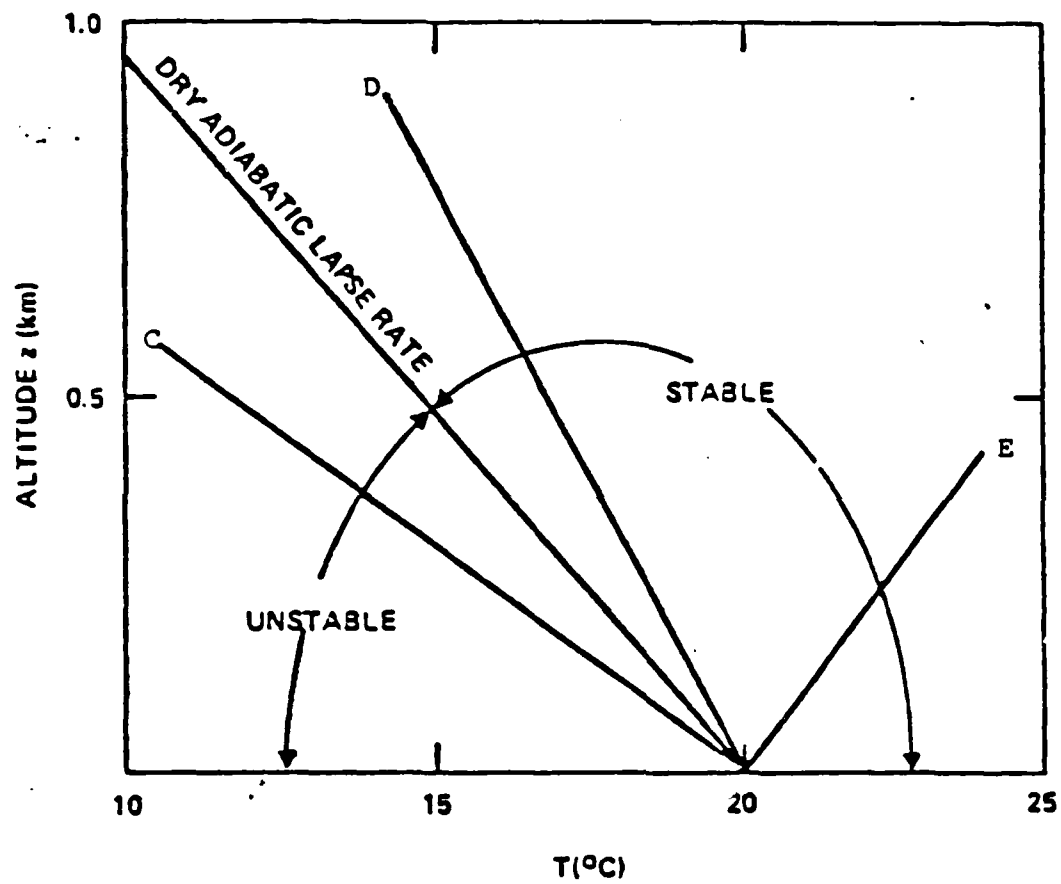


Figure 2.2

Temperature Profiles indicating lapse rates:
Slightly Unstable (C), Neutral (Dry Adiabatic), Neutral (D),
and Slightly Stable (E).

Table 2.1

Stability Classification by $\Delta T/\Delta Z$

CLASS	ΔT IN °C/100 METERS	DEFINITION
A	Less than -1.9	Extremely unstable
B	-1.7 to -1.9	Unstable
C	-1.5 to -1.7	Slightly unstable
D*	-0.5 to -1.5	Neutral
E	-0.5 to 1.5	Slightly stable
F	1.5 to 4.0	Stable
G	Greater than 4.0	Extremely stable

To accomplish this, 2 two-dimensional hydrodynamic models are presented. These allow a velocity profile to be present in the wind field and account for buoyancy terms due to density variations.

2.2.1 Axi-symmetric Dispersion Model

In a calm (or near calm) environment, axi-symmetric flow should be assumed in analyzing the air entrainment and dispersion effects of the well-defined round vapor cloud. In a cylindrical coordinate system, the governing equations of the time averaged mean flow variables are:

Conservation of Mass:

$$(9) \quad \frac{1}{r} \frac{\partial}{\partial r}(rv_r) + \frac{\partial v_z}{\partial z} = 0$$

Conservation of Momentum:

$$(10) \quad \frac{\partial v_r}{\partial t} + v_r \frac{\partial v_r}{\partial r} + v_z \frac{\partial v_r}{\partial z} = - \frac{1}{\rho_0} \frac{\partial p}{\partial r} + \frac{1}{r} \frac{\partial}{\partial r} \left(r K_m \right) \frac{\partial v_r}{\partial r}$$

$$(11) \quad \frac{\partial v_z}{\partial t} + v_r \frac{\partial v_z}{\partial r} + v_z \frac{\partial v_z}{\partial z} = - \frac{1}{\rho_0} \frac{\partial p}{\partial z} + \left(\frac{\rho}{\rho_0} - 1 \right) g$$

$$+ \frac{1}{r} \frac{\partial}{\partial r} \left(r K_m \frac{\partial v_z}{\partial r} \right) + \frac{\partial}{\partial z} \left(K_m \frac{\partial v_z}{\partial z} \right)$$

Conservation of Energy:

$$(12) \quad \frac{\partial \bar{T}}{\partial t} + v_r \frac{\partial \bar{T}}{\partial r} + v_z \frac{\partial \bar{T}}{\partial z} = -v_z \left(\Gamma + \frac{\partial T_o}{\partial z} \right) + \nabla \cdot K_T \nabla \bar{T}$$

$$(13) \quad \frac{\partial c}{\partial t} + v_r \frac{\partial c}{\partial r} + v_z \frac{\partial c}{\partial z} = \nabla \cdot K_c \nabla c$$

where

v_r = radial velocity

v_z = axial velocity

p = pressure

K_m, K_c, K_T = momentum, concentration, and thermal
diffusivities

ρ = density

ρ_o = ambient density

g = gravitational constant

T = temperature

T_o = ambient temperature

$\bar{T} = T - T_o$

Γ = adiabatic lapse rate

c = concentration

t = time

In order to eliminate pressure terms in the momentum equation, the vorticity determination is introduced into the problem as:

$$(14) \quad \eta = \frac{\partial v_r}{\partial z} - \frac{\partial v_z}{\partial r}$$

By cross differentiating and subtracting the momentum equations (10) and (11), and using the conservation of mass equation, (9), one is able to derive an equation governing the vorticity as:

$$(15) \quad \frac{\partial \eta}{\partial t} + v_r \frac{\partial \eta}{\partial r} + v_z \frac{\partial \eta}{\partial z} + \eta \left(\frac{\partial v_r}{\partial r} + \frac{\partial v_z}{\partial z} \right) = \frac{\partial}{\partial r} \left(K_m \frac{\partial \eta}{\partial r} \right) + \frac{\partial}{\partial z} \left(K_m \frac{\partial \eta}{\partial z} \right) - K_m \frac{\eta}{r^2} - \frac{g}{\rho_0} \frac{\partial \rho}{\partial r}$$

Now two stream function ψ can be introduced to satisfy the continuity equation (9):

$$(16) \quad v_r = \frac{1}{r} \frac{\partial \psi}{\partial z}$$

$$(17) \quad v_z = - \frac{1}{r} \frac{\partial \psi}{\partial r}$$

Through the definition of vorticity, the stream function will satisfy the following equation:

$$(18) \quad \frac{\partial^2 \psi}{\partial z^2} + \frac{\partial^2 \psi}{\partial r^2} - \frac{1}{r} \frac{\partial \psi}{\partial r} = r \eta$$

This concludes the system of equations governing the dispersion of an axi-symmetric cloud in quiescent environment.

Quasi-Three Dimensional Dispersion Model

This model follows a specific slice of air as it moves downwind under the influence of a mean wind flow. The hydrodynamic equations expressing the conservation of mass, momentum, and energy together with a Boussinesq approximation for the atmosphere are written in rectangular coordinates. In a coordinate system such that x is the downwind direction, y is the crosswind direction, and z is the vertical direction, these equations are:

Conservation of Mass

$$(19) \quad \frac{\partial u}{\partial x} + \frac{\partial v}{\partial y} + \frac{\partial w}{\partial z} = 0$$

Conservation of Momentum

$$(20) \quad \frac{Du}{Dt} = - \frac{1}{\rho_0} \frac{\partial p}{\partial x} + \nabla \cdot (K_m \nabla u)$$

$$(21) \quad \frac{Dv}{Dt} = - \frac{1}{\rho_0} \frac{\partial p}{\partial y} + \nabla \cdot (K_m \nabla v)$$

$$(22) \quad \frac{Dw}{Dt} = - \frac{1}{\rho_0} \frac{\partial p}{\partial z} + \frac{\rho}{\rho_0} g + \nabla \cdot (K_m \nabla w)$$

Conservation of Energy

$$(23) \quad \frac{DT}{Dt} = - \frac{1}{C_p} w g + \nabla \cdot (K_T \nabla T)$$

Conservation of Species

$$(24) \quad \frac{Dc}{Dt} = \nabla \cdot (K_c \nabla c)$$

where

$$\frac{D}{Dt} = \frac{\partial}{\partial t} + u \frac{\partial}{\partial x} + v \frac{\partial}{\partial y} + w \frac{\partial}{\partial z}$$

u, v, w = velocity components in the x, y, z directions, respectively.

If the assumption is made that the downwind velocity is independent of position and unmodified by the addition of the plume, the momentum equation in the x direction can be omitted (it is assumed to be satisfied by the mean atmosphere motion and u is independent of x). The equations reduce to:

$$(25) \quad \frac{\partial v}{\partial y} + \frac{\partial w}{\partial z} = 0$$

$$(26) \quad u \frac{\partial v}{\partial x} + v \frac{\partial v}{\partial y} + w \frac{\partial v}{\partial z} = - \frac{1}{\rho_0} \frac{\partial p}{\partial y} + \nabla \cdot (K_m \nabla v)$$

$$(27) \quad u \frac{\partial w}{\partial x} + v \frac{\partial w}{\partial y} + w \frac{\partial w}{\partial z} = - \frac{1}{\rho_0} \frac{\partial p}{\partial z} - \frac{\rho g}{\rho_0} + \nabla \cdot (K_m \nabla w)$$

$$(28) \quad u \frac{\partial T}{\partial x} + v \frac{\partial T}{\partial y} + w \frac{\partial T}{\partial z} = - w \frac{g}{C_p} = \nabla \cdot (K_T \nabla T)$$

$$(29) \quad u \frac{\partial c}{\partial x} + v \frac{\partial c}{\partial y} + \frac{\partial c}{\partial z} = \nabla \cdot (K_c \nabla c)$$

By cross-differencing and subtracting the momentum equations and using the conservation of mass equation, one is able to reduce the number of equations to be solved by one. Defining a vorticity by:

$$(30) \quad \eta = \frac{\partial v}{\partial z} - \frac{\partial w}{\partial y}$$

and using the momentum equations which have been reduced to eliminate the pressure terms yields a vorticity equation:

$$(31) \quad u \frac{\partial(\eta)}{\partial x} + \frac{\partial(v\eta)}{\partial y} + \frac{\partial(w\eta)}{\partial z} = \frac{g}{\rho_0} \frac{\partial \rho}{\partial y} + \nabla \cdot (K_m \nabla \eta)$$

Since $\nabla \cdot \vec{v} = 0$, there exists a stream function ψ such that:

$$(32) \quad v = \frac{-\partial \psi}{\partial z} \quad w = \frac{\partial \psi}{\partial y}$$

combining the stream function definition with the vorticity definition resulted in a Poisson equation relating the vorticity to the stream function.

$$(33) \quad \nabla^2 \psi = \eta$$

where

$$\nabla^2 = \frac{\partial^2}{\partial y^2} + \frac{\partial^2}{\partial z^2}$$

The density variations are written in terms of a temperature and concentration variation in the Boussinesq approximation resulting in a final set of equations as follows:

$$(34) \quad \frac{\partial(\eta)}{\partial x} + \frac{1}{u} \frac{\partial(v\eta)}{\partial y} + \frac{\partial(w\eta)}{\partial z} = \frac{g}{\rho_0 u} \frac{\partial \rho}{\partial y} + \frac{\nabla \cdot (K_m \nabla \eta)}{u}$$

$$(35) \quad \frac{\partial \bar{T}}{\partial x} + \frac{1}{u} \frac{\partial (v\bar{T})}{\partial y} + \frac{\partial (w\bar{T})}{\partial z} = -\frac{w}{u}\Gamma + \frac{\nabla \cdot (K_T \nabla \bar{T})}{u}$$

$$(36) \quad \frac{\partial c}{\partial x} + \frac{1}{u} \frac{\partial (vc)}{\partial y} + \frac{\partial (wc)}{\partial z} = \frac{\nabla \cdot (K_c \nabla c)}{u}$$

The specific relationship between density, temperature, and concentration will depend upon the equation of state used. Typically a mixture equation is used where:

$$(37) \quad \rho = (1-C) \rho_0 + C\rho_c$$

ρ_0 = density of air

ρ_c = density of added constituent

The individual densities are assumed to obey a perfect gas law.

2.3 Results

2.3.1 Literature Review

A review of the literature associated with the use of aircraft fuels and methods of cleaning up spills was completed as a portion of this project. The information collected during this literature survey has resulted in information on the size of liquid pools as a function of spill size, some limited information on the frequency of fuel spills in the Air Force and a body of literature associated with the dumping of JP4 in the atmosphere and the resulting vaporization of the fuel. This data has provided some insight into the important parameters for the modeling effort. Appendix E summarizes the specific data utilized in the modeling effort undertaken in this study.

Cicccone and Graves (1) completed a study of the frequency of spills and looked at means of mitigation associated with these spills. Table 2.2 presents the results of their limited study on fuel spills at Air Force facilities. This data indicates that spills of the smallest size do occur approximately 10 to 15 times more frequently than the larger spills. However, the data indicate that on the average one large spill occurs each month at each Air Force operating facility. This frequency is such that consideration should be given to the associated flammable cloud problem and the procedures that are in effect in the vicinity of the spill. A knowledge of the hazard posed by these spills is important in determining what maintenance procedures or other activities can occur in the vicinity of an aircraft being refueled. The ability to conduct simultaneous activities with aircraft being refueled could significantly decrease the "turn around" time for an aircraft.

TABLE 2.2
SUMMARY OF AVERAGE SPILL FREQUENCY
(spills/month)

No. of Sample Bases	Small (0-4 gallons)	Medium (5-42 gallons)	Large (>42 gallons)
23	15.95	4.93	.91
37	13.79	5.11	1.22

2.3.2 Liquid Spill Model Results

A series of calculations were made for different size pools and different environmental conditions. The results of the model runs indicate that the vapor generation rate from the pool quickly drops to a steady state value that is a function of the mass transfer from the pool and the heat transfer to the pool from the surroundings. Figure 2.3 is a plot of the calculated vapor source rate for a 40 gallon JP4 spill with the fuel and ground temperature at 20 C and the wind speed of 5 miles per hour. As one can see the vaporization rate is essentially constant. This is caused because the steady state solution is a balance between heat into the pool from the ground and heat loss because of the material be evaporated. Steady state is reached in a short time compared with the total time for the liquid pool to be evaporated.

Table 2.3 shows the steady state rate of vapor generation for other sizes and environmental conditions. Because of the model assumption of a constant pool thickness, the pool diameter is directly related to the volume of material spilled. For the 40 gallon spills the pool diameter is 19.6 meters and for the 4 gallon spills the pool diameter is 6.2 meters. The vapor source rate behaves as one would expect. As wind speed and fuel temperature are increased the vapor rate is increased. As the free stream vapor pressure is increased the vapor rate is decreased. Since the vapor rate is almost constant the time to vaporize the spill increases as the vaporization rate decreases.

The results of the liquid spill modeling calculations indicate that the vapor source rate for a 40 gallon spill can vary by almost an order of magnitude, depending on the assumed environmental conditions existing at the time of the spill. This type of result is typical of releases to the atmosphere where the ambient environment significantly influences the results. The other significant result from these calculations is that the

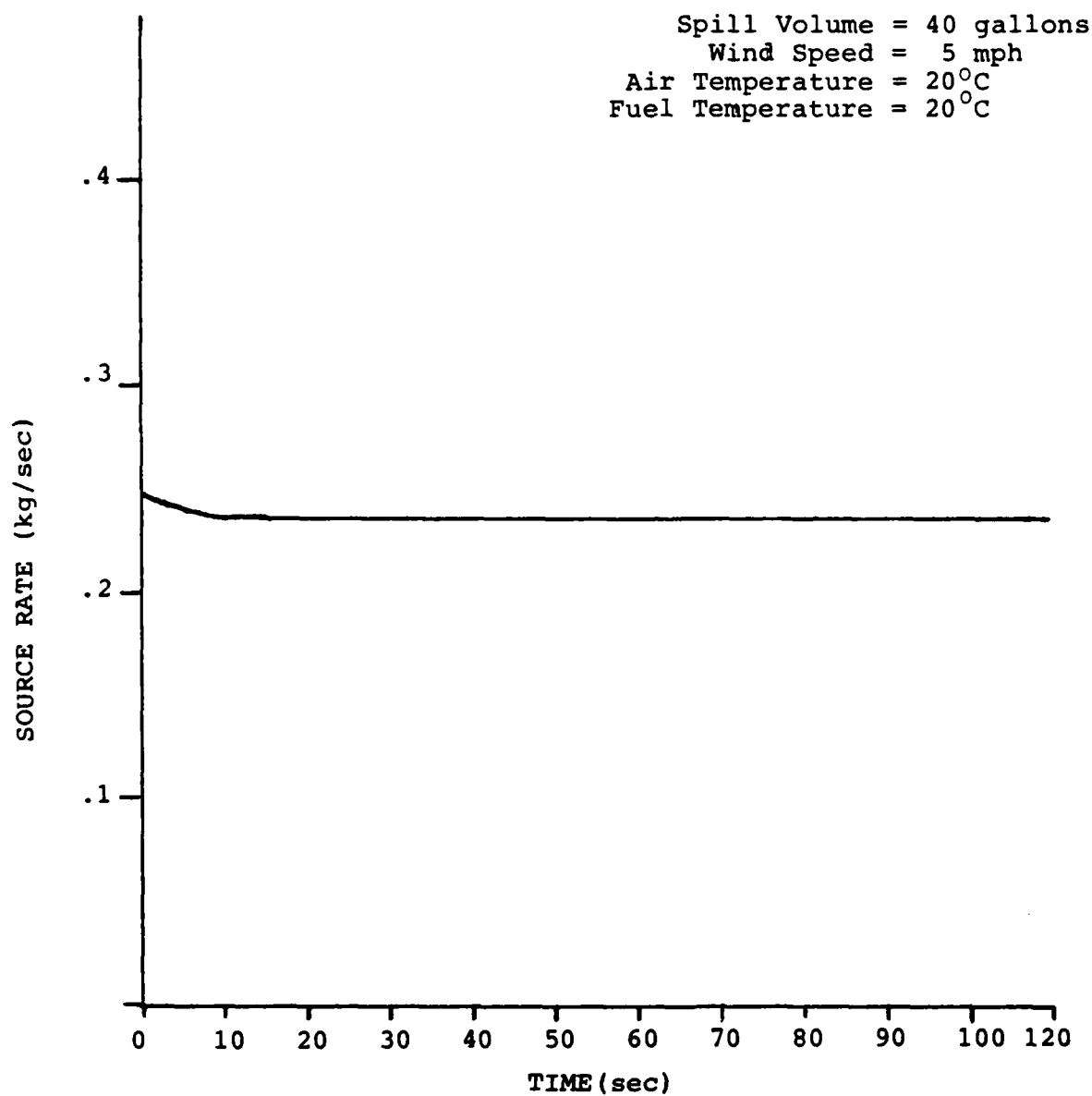


Figure 2.3
POOL VAPORIZATION RATE

TABLE 2.3

SUMMARY OF LIQUID SPILL RESULTS

SPILL SIZE (gal)	WIND SPEED (mph)	AIR TEMP. (°C)	FUEL TEMP. (°C)	$\frac{P_{\infty}}{P}$	VAPOR RATE (kg/sec)	VAPOR TIME (sec)
40	10	20	20	.755	.4045	285
40	5	20	20	.755	.2375	450
4	5	20	20	.755	.0269	425
40	5	40	20	.755	.3802	300
40	5	20	0	.755	.1477	770
40	1	40	20	0	.4145	280
40	1	20	20	0	.2653	430
40	5	20	20	0	.8711	130

vapor source rate is essentially constant and could be assumed constant for the purpose of hazard estimation.

2.3.3 Spray Model Results

The question of droplet distribution resulting from a break in a pressurized fuel line is not well known. The size of droplets produced would be limited on the large end by the size of the hole in the pressurized line. The small droplets size will be determined by the stability of the larger droplets and the breakup of these droplets. During this phase of the project it was impossible to determine what the droplet distribution should be, therefore some limited calculations were made on specific droplets.

Table 2.4 provides the results from several different calculations of droplet behavior. Calculations were made for droplets from 200 micron diameter to 4000 micron diameter. The release velocity was assumed to be constant and typical of the initial velocity that would result from a hole in a 50 psi pressurized line. All of the calculations were made assuming a release location on the ground and that the drop would travel upward and then return to the ground again.

As would be expected the larger droplets travel significantly further than the smaller droplets. The distance varies from less than one meter to approximately 15 meters. Thus the spray distance could reach as far as 50 feet from the release location. The loss of material due to vaporization from the droplets is very small. For all of the cases considered, less than 5% of the material in the drop would be evaporated before the droplet reached the ground.

It is of interest to compare the vaporization from the single component droplet used in the model presented in this study with the multi-component model presented by Clewell (7) that was

TABLE 2.4
SUMMARY OF DROPLET MODEL RESULTS

DROPLET DIAMETER (microns)	RELEASE ANGLE	RELEASE VELOCITY (m/sec)	HORIZONTAL DISTANCE (m)	MAXIMUM HEIGHT (m)	% LOSS
200	45	30	.72	.315	4.5
1000	45	30	5.25	2.70	5.0
2000	45	30	9.40	4.61	3.8
3000	45	30	12.8	6.05	3.1
3000	55	30	12.14	6.78	3.2
3000	35	30	13.1	5.04	2.9
4000	45	30	16.0	7.20	2.7

developed for calculation of evaporation of JP4 jettisoned by aircraft. Because the problems are significantly different in formulation the only comparison of significance is the amount of vaporization that occurs in the first few meters. For a 1000 micron diameter droplet the multi-component model predicts that 11% would be vaporized in 3 meters and 13% in five meters. This result is 2 to 3 times as large as that predicted by the single component model and is because the lighter components evaporate more rapidly than the model of this study predicts. This area will require more investigation during the proposed phase II program.

2.3.4 Dispersion Model Results

Table 2.5 shows the results of three calculations made with the Disco Model using the source rate for 40 gallon spills of JP-4. A range of parameters were selected so that information would be gained on the range of expected regions where the flammable hazard would be expected. These results are extended to the point where the mean concentration predicted by the model is below the lower flammable limit of 1.3% JP-4 in air. The sources selected for these calculations represent conditions that would cause the maximum downwind distance to occur. A stable category of F was selected for each of the calculations and the wind speeds were selected toward the lower end of wind speeds.

The results show that the maximum hazard distances occur at low wind speeds and stable conditions. The distances predicted by the model are very short with the maximum being only slightly over 7 meters downwind of the source. The vapor rates predicted by the droplet or spray model also yield similarly short distances.

If calculations had been made over a range of parameters for stability and wind speed, the resulting distances would have been significantly shorter than those presented. There are however,

TABLE 2.5

SUMMARY OF DISPERSION MODEL RESULTS

SOURCE RATE (KG/SEC)	WIND SPEED (M/SEC)	STABILITY CLASS	DOWNWIND DISTANCE (M)
.4145	1.0	F	7.05
.8711	5.0	F	1.17
.3802	5.0	F	0.45

several unknowns which need to be answered to determine if these distances are realistic. The model in its present form assumes that the turbulent diffusivity of the atmosphere is constant near the ground. There exist theoretical arguments for this diffusivity that would have it significantly decrease near the ground. This decrease in diffusivity could result in somewhat longer distances. The proposed Phase II measurement program would address this question.

In summary the model results indicate that the flammable cloud will exist only very near the source and that the possibility of a fire being started more than a few meters away from a liquid pool or a region where liquid spray exists is very remote.

3.0 CONCLUSIONS AND RECOMMENDATIONS

The results of this phase I study indicate that the current procedures and restrictions on activities during the refueling of aircraft may in many ways be too restrictive. Models were developed for consideration of the typical kinds of JP-4 releases that can occur and estimates of the extent of the flammable hazard area associated with these releases were made. These estimates indicate that the area of concern is limited to the near proximity of liquid spills or the region where droplet sprays may reach. The vaporization rate of JP-4 is such that the evolved vapor cloud will be diluted below the lower flammable limit within a few meters of the source.

Estimates of the liquid pool size indicate that for a 40 gallon spill the pool size may be as large as 20 meters in diameter so that the hazard distance slightly greater than 30 feet from the pool center if a short dispersion distance is added for the vapor cloud. Similarly, the calculations of spray distance indicate that travel distance for the droplets would be between 10 and 15 meters. This results in a hazard distance of from 30 to 45 feet. Both of these projected distances are less than the 50 foot distance presently utilized for safety purposes.

Several parameters were found which are not well known for the releases under consideration. Data does not exist that documents these parameters in detail and further research is needed to determine these parameters. All of these parameters do influence the model predictions and can influence the conclusions. The parameters considered to be of significant importance are as follows:

- Dispersion parameters (eddy diffusivities) within one or two pool diameters as a function of measured meteorological conditions

- Droplet size distribution associated with the rupture of refueling lines or pressurized tanks
- Drag coefficient associated with an evaporating droplet
- Liquid pool thickness and spread rate
- Vapor pressure variation over a liquid pool or surrounding a liquid drop moving through the atmosphere
- Determination of evaporation rate to determine if single component model is satisfactory

These six parameters are those that are the most questionable and could influence the model predictions by a change in the parameter value. A thorough knowledge of these parameters will provide the assurance that the model predictions are reasonable. For those portions of the model where data was available, comparisons have been made and agreement was excellent. In other areas, no data is available and assumptions have been required.

During phase I of this study, Tracer Technologies met all technical objectives by developing two source rate and two atmospheric dispersion models specifically designed to predict the hazards associated with JP4 fuel spills. Additionally, limited exercise of the models, which indicate hazard distances much smaller than those implied by existing safety standards, resulted in the identification of key parameters which need further definition to provide models which have significant credibility. Phase II of this study is designed to assure that all the key parameters have been identified and that values are determined through an experimental program that assure these parameters are accurately represented. In addition, the experimental program would provide measurements on actual spills that would provide the necessary verification of the model results. No spills of JP-4 have been conducted to determine the

hazard distance and this necessary effort will need to be undertaken to show that the model results are in agreement with actual measurements.

The proposed Phase II study will consist of (1) additional model calculations to define the experimental program, (2) design and conduct of JP-4 spills at Kirtland Air Force Base, (3) modification of the existing models utilizing the results from the measurement program, (4) merge the models into a complete package, (5) develop simplified models (nomographs or calculator models) for use in the field and (6) conduct some final "hands-off" validation experiments to show that the models work properly. This program will provide the Air Force with a working documented package for use in evaluation of fuel spill hazards.

REFERENCES

REFERENCES

1. Ciccone, V.J. and A.P. Graves, "A Study to Evaluate the Intensity of Alternative Methods for Neutralization of DOD Aircraft Fuel Spills." DOD Aircraft Ground Fire Suppression and Rescue Office, AD-A025937, Feb. 1976.
2. "Handbook of Aviation Fuel Properties", CRC Report 530, Society of Automotive Engineers, Inc., Warrendale, Pa., 1983.
3. Mackay, D. and R.S. Matsugu, "Evaporation Rates of Liquid Hydrocarbon Spills on Land and Water", The Canadian Journal of Chemical Engineering, Vol. 51, August, 1973.
4. Dawbarn, R., K.W. Nutt, and C.W. Pender, "A Study of the Jettisoning of JP-4 Fuel in the Atmosphere", Arnold Engineering Development Center, AEDC-TR-75-49, AD-A017555, Nov. 1975.
5. Sutton, O.G., "Micrometeorology", McGraw Hill, New York, 1953.
6. Eckert, E.R.G. and R.M. Drake, "Heat and Mass Transfer", McGraw-Hill, New York 1959.
7. Clewell, Harvey J., "Evaporation and Groundfall of JP-4 Jet Fuel Jettisoned by USAF Aircraft", Engineering & Services Laboratory, Tyndall Air Force Base, Fla., Report ESL-TR-80-56, AD-A109307, Sept. 1980.

Appendix A

POOL

Pool is a small program that solves the heat and mass transfer equations for a well mixed liquid pool to determine the vapor rate as a function of time. The primary dependent variable is the pool temperature which is advanced in time by an explicit differencing scheme utilizing equation as the basis for the differencing scheme. The only temperature dependent parameter in the calculation.

The program consists of three routines: DRIVER, POOL, VPRESS. DRIVER is an interactive routing that asks for the problem specific input data, POOL solves the differential equation and computes the time varying parameters of the problem and VPRESS provides the vapor pressure of JP4 as a function of temperature. Figure A-1 is a flowchart of the POOL source model. The subroutines of the POOL model are relatively straight forward. Each routine is briefly described below.

Routine DRIVER

This is the main routine of the model. It is interactive and asks the user for the required input compute the vapor source rate for a specific problem. The necessary input is (1) spill volume in gallons, (2) windspeed in mph (3) the ambient air temperature in °C and (4) the spilled fuel temperature in °C.

Subroutine POOL

Subroutine POOL does an energy calculation of the liquid pool and computes the rate at which vapor is evolved from the liquid pool. The outputs from this model are (1) the time in sec after the spill, (2) the liquid temperature, (3) the evaporation rate in kg/sec and (4) the remaining pool mass in kg.

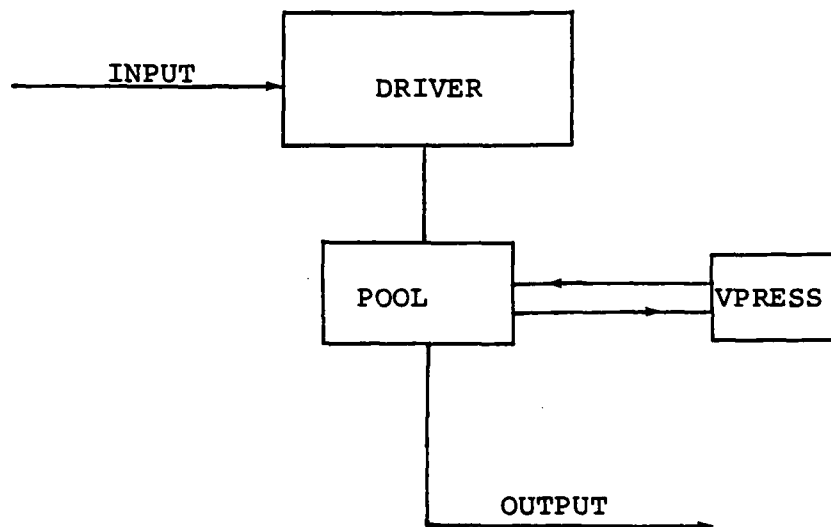


Figure A-1
Flowchart POOL Sources Model

Subroutine VPRESS

This is a curve-fit routine which returns the vapor pressure of JP4 as a function of temperature.

MAIN VARIABLES OF POOL MODEL

AP = area of pool
C = constant in evaporation equation
CPL = liquid specific heat
CPV = vapor specific heat
COND = heat conduction from ground
DELT = time step
DELH = heat of vaporization
PRAD = pool radius
PMASS = liquid pool mass
PVAP = vapor pressure of JP4
RAD = radiation heat transfer
RED = ratio of ambient vapor pressure to saturation value
RHOV = vapor density
RMASS = mass evaporation rate
SPILV = volume of spill
SOLAR = solar radiation constant
TAMB = ambient temperature
TL = liquid temperature
VAPOR = heat transfer from vapor

Appendix B

DROP

DROP is a small interactive program that solves the dynamic behavior of a single droplet as well as solving the integral heat and mass transfer equations around the drop. Thus the model keeps track of the droplet trajectory as well as computes the changing size of the droplet due to mass transfer from the droplet. The primary dependent variables in the equation are the x,y positions of the droplet, the corresponding velocities of the droplet and the temperature of the droplet.

The equations of motion and the coupled energy equation are integrated numerically in an explicit method which uses current values of temperature, velocity and position to compute the rate at which these parameters change and their updates each of the parameters. The equations are coupled because the radius of the droplet is decreasing due to mass loss and the drag force on the droplet is a function of the radius. In addition the velocity of the droplet affects the heat and mass transfer rates.

The program consists of four routines: DROP, QUAD, EVAP, & VPRESS. DROP is the main routine it asks for input and computes the marching in time. EVAP computes the mass transfer rate from the droplet. QUAD is a quadratic equation solver and VPRESS is a fitting routine that provides the vapor pressure as a function of temperature. Figure B-1 is a flowchart of the DROP source model.

The subroutine of the DROP model are relatively straight forward. Each routine is briefly described below.

Routine DROP

This is the main routine of the model. It is interactive and requires input from the user. The input required is as follows: (1) the initial drop radius, (2) the angle the droplet trajectory makes with the ground, (3) the initial velocity of the droplet, (4) the ambient air temperature and (4) the initial temperature of the fuel drop. Utilizing this input data the equations of

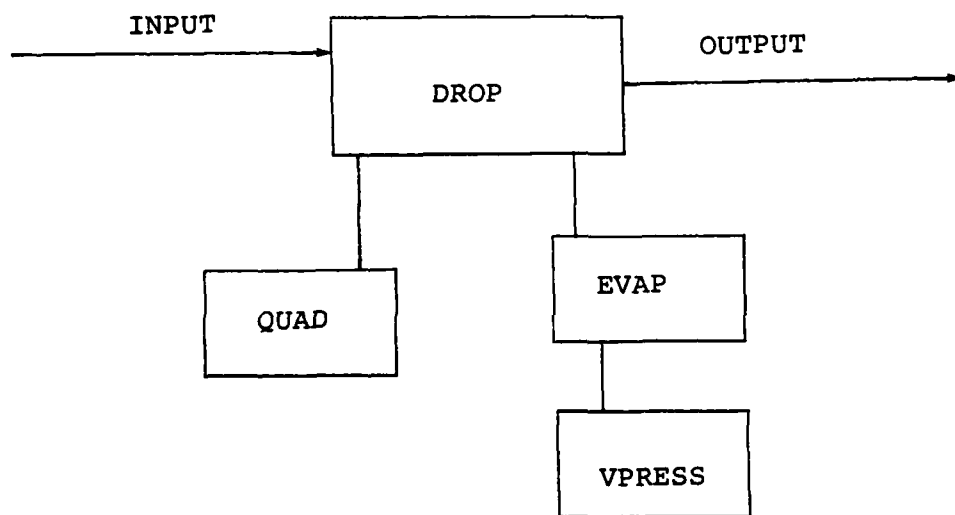


Figure B-1
Flowchart DROPLET Source Model

motion are then integrated to determine the dynamic behavior of the drop.

The output information provided by the model is (1) the X,Y position where X is the horizontal position and Y is a vertical position of the drop, (2) the time after release of the drop, (3) the U,V velocities corresponding to the X,Y directions, (4) the mass of the droplet and (5) the evaporation rate from the droplet.

Subroutine QUAD

QUAD is a small routine that solves a second order algebraic equation for the velocities of the drop at each time step.

Subroutine EVAP

EVAP is a routine that integrates the energy equation for the droplet and determines the evaporation rate for the droplet.

Subroutine VPRESS

VPRESS is a curve-fit routine which returns the vapor pressure of JP-4 as a function of temperature.

MAIN VARIABLES OF POOL MODEL

ANG = initial droplet elevation angle of trajectory
ATEMP = ambient temperature
C = constant in evaporation equation
CPL = liquid specific heat
CPV = vapor specific heat
DELT = time step
DELH = heat of vaporization
FTEMP = initial droplet temperature
PMASS = droplet mass
PVAP = vapor pressure of JP4
RAD = radiation heat transfer
RED = ratio of ambient vapor pressure to saturation value
RHOV = vapor density
RDOT = mass evaporation rate
TIME = time of simulation
TA = ambient temperature
TL = liquid temperature
U = horizontal velocity
V = vertical velocity
VAPOR = heat transfer from vapor
X = horizontal position
Y = vertical position

Appendix C

AXISYM

For numerical solution, equation 12 may be written in the form:

$$\begin{aligned}
 (C-1) \quad \frac{\partial \eta}{\partial t} + \frac{\partial}{\partial r} (v_r \eta) + \frac{\partial}{\partial z} (v_z \eta) = \frac{\partial}{\partial r} \left(K_m \frac{\partial \eta}{\partial r} \right) \\
 + \frac{\partial}{\partial z} \left(K_m \frac{\partial \eta}{\partial z} \right) - K_m \eta / r^2 - \frac{q}{\rho_o} \frac{\partial \rho}{\partial r}
 \end{aligned}$$

The advection terms in (C-1) are solved using the Crowley 2nd order scheme (5) and a centered second difference (9) is used on the horizontal and vertical diffusion terms. The non-differential term is evaluated at the previous time step and the density gradient is found from a standard first order cell centered difference.

Crowley Second Order Scheme

The advection terms in equation (C-1) are in the form:

$$(C-2) \quad \frac{\partial \phi}{\partial t} + \frac{\partial \phi u}{\partial x} = 0$$

Let

$$(C-3) \quad \phi^{n+1} = \phi^n - (F_{j+1/2} - F_{j-1/2})$$

where

$$F_{j+1/2} = \alpha_{j+1/2} (\phi_{j+1} - \phi_j) - \alpha_{j+1/2}^2 (\phi_{j+1} - \phi_j)/2$$

and

$$\alpha_{j+1/2} = u_{j+1/2} \Delta t / \Delta x$$

Centered Second Difference Scheme

The diffusion terms in equation (17) are in the form:

$$(C-4) \quad \frac{\partial \phi}{\partial t} = \frac{\partial}{\partial x} \left(x \frac{\partial \phi}{\partial x} \right)$$

Let

$$(C-5) \quad \phi^{n+1} = \phi^n - (F_{j+1/2} - F_{j-1/2}) / \Delta x$$

where

$$F_{j+1/2} = \Delta t K_{j+1/2} (\phi_{j+1} - \phi_j) / \Delta x$$

and the K's are interface quantities.

Stream Function Calculation

Equation (15) is solved by a successive over-relaxation method. The spacial difference mesh being solved is given by:

$$\begin{aligned} (C-6) \quad & \frac{\psi_{i+1,j} - 2\psi_{i,j} + \psi_{i-1,j}}{(\Delta r)^2} + \frac{\psi_{i,j+1} - 2\psi_{i,j} + \psi_{i,j-1}}{(\Delta z)^2} \\ & + \frac{1}{r_i} \frac{\psi_{i,j} - \psi_{i-1,j}}{2\Delta r} = \frac{1}{4} [r_i (\eta_{i,j} + \eta_{i,j-1}) + \\ & r_{i-1} (\eta_{i-1,j} + \eta_{i-1,j-1})] \end{aligned}$$

Convergence is expedited by over-relaxing in $\psi_{i,j}$ of the Mth iteration with the following:

$$(C-7) \quad \psi_{i,j} = \Omega \psi_{i,j}^M + (1-\Omega) \psi_{i,j}^{M-1}$$

where

$\Omega = \text{constant}$

It was found that convergence is most rapid with $\Omega = 1.5$.

With the stream function determined the velocities are easily calculated by:

$$(C-8) \quad \Omega_{r,i,j} = \frac{1}{r_i} \frac{\psi_{i,j+1} - \psi_{i,j-1}}{2\Delta z}$$

and

$$(C-9) \quad \Omega_{z,i,j} = \frac{-2}{(r_i + r_{i+1})} \frac{\psi_{i+1,j} - \psi_{i-1,j}}{2\Delta r}$$

AXISYM (AXI-Symmetric Dispersion Model)

AXISYM is a group of subroutines that uses the data produced by the various source models in HAZARD and performs a dispersion calculation which is dominated by the gravity spread of the evolved cloud. Figure c-1 is a schematic diagram of the overall logic used in the AXISYM program.

The first subroutine called is ASTART which relates the variables from HAZARD with the variables used in AXISYM. AXISYM then enters a loop which advances the simulation in time. Inside of the loop at each time-step, the following routines are called: ITLAPL, VEL, SETDIF, FIXUP, DELTAT, OUT1, and REZONE. These routines calculate the stream function, velocities, diffusivities, and then update the vorticities in each zone. A new time-step is calculated and data is printed which documents the changing nature of the cloud.

The cyclic behavior continues until the cloud concentration is below the flammable limit and/or the 100ppm H_2S toxic limit. A brief description of each subroutine is described in the following section. Due to the similarities between the routines used for DISCO and AXISYM, the reader is referred to the flow diagram of the corresponding routine in DISCO.

Subroutines of AXISYM

Subroutine ASTART

ASTART initializes the variables and arrays for the beginning of the calculation. Several constants and parameters are also calculated in this subroutine. (see Figure D-2 ; INPUT1)

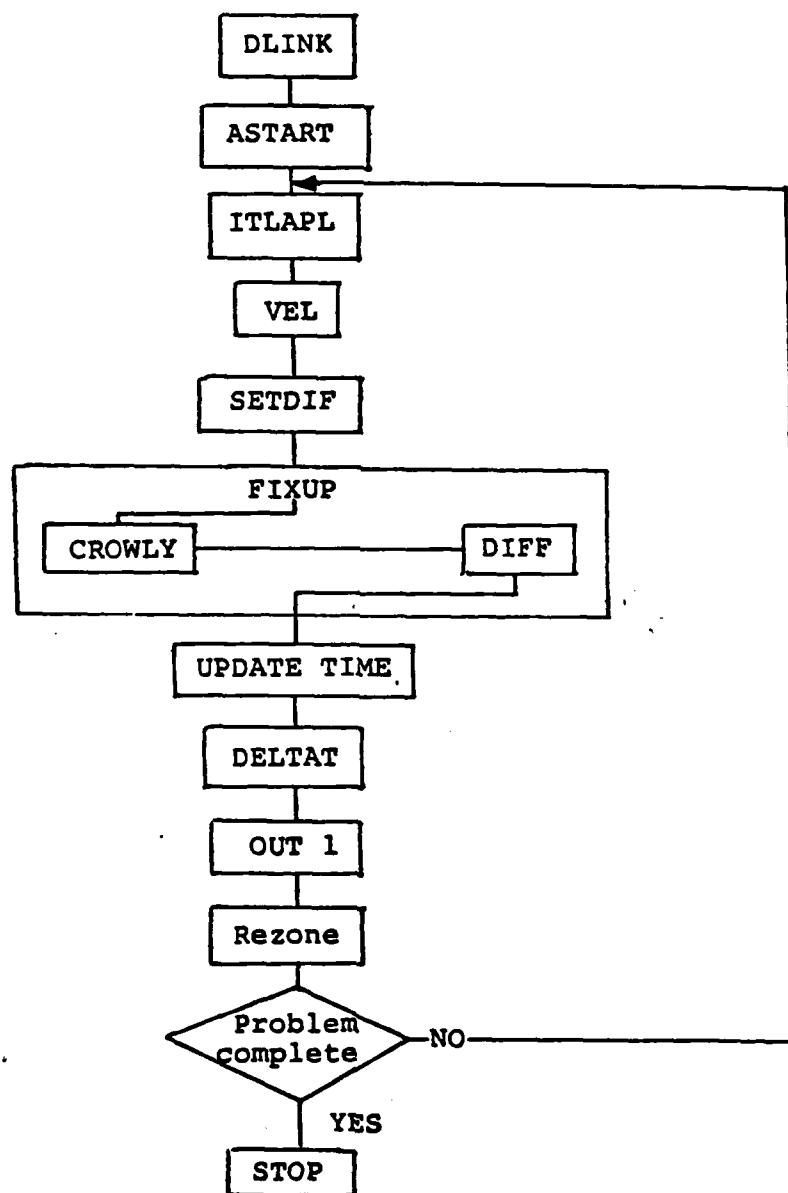


Figure C-1 Flowchart AXISYM Dispersion Model

Subroutine ITLAPL

ITLAPL iteratively solves the Poisson equation for the stream function using an over-relaxation method. ITLAPL calls source to determine the boundary conditions on the stream function that will allow the correct gas volume to flow into the grid.

Subroutine VEL

VEL calculates the horizontal and vertical velocity throughout the grid from the stream-function array.

Subroutine SETDIF

SETDIF uses the local velocity and temperature stratification in each zone to determine the horizontal and vertical diffusivities throughout the grid. These diffusivities are updated on each cycle of the calculation. (see Figure D-3 ; SETEV)

Subroutine FIXUP

FIXUP is the subroutine where the conservation equations for mass, energy, and vorticity are updated. These updates are done by considering diffusion, advection, and other terms such as the buoyancy and source terms. The advective updates are accomplished in subroutine DIFF. For the concentration and temperature, a variable transformation is accomplished by multiplying by the local radius before calling CROWLY and DIFF. (see Figure D-5 ; UPDATE)

Subroutine OUT1

OUT1 is the output routine where information on the cloud size and shape is provided to the user.

Subroutine REZONE

REZONE is a routine that provides the capability to enlarge the region of interest. When the disturbance approaches the boundary of the grid, then the horizontal or vertical zone size is doubled and new ambient regions are added around the disturbance. (see Figure D-8)

Main Program Variables for AXISYM

C - concentration array (v/v)
C1 - change in concentration array during time step (v/v)
CAMB - initial concentration (v/v)
CBOU - concentration of source gas
CPMETH - average specific heat of gas (J-KG/°K)
DT - time step (sec)
DTS - initial time step (sec)
DX - horizontal zone size (m)
DY - array of vertical zone sizes
DYBOTM - vertical height of bottom zone (M)
EVX - radial diffusivity array (M^2/sec)
EVY - vertical diffusivity array (M^2/sec)
G - gravity (9.8 M/sec)
GAMMA - adiabatic lapse rate (°K/100 meters)
HEATC - surface, heat transfer coefficient
ICYCL - cycle number
ILONCE - initialization flag for ITLAPL
ISONCE - initialization flag for SETDIF
IZONE - IZONE is initialization flag for REZONE
NCYCLS - total number of cycles in problem
NX - number of zones
NXM1 - NX-1
NXM2 - NX-2
NXPI - NX+1
NY - number of vertical zones
NYM1 - NY-1
NYM2 - NY-2
NYP1 - NY+1
ODT - previous time setp (sec)
P - stream function (M^3/sec)
PRMETH - pressure divided by specific gas constant
R2DX - $1/(2*\Delta X)$
RDX - $1/DX$

RDX2 - $1/(DX)^2$
 RX - array of radial distance to inner zone boundary
 RXMIDI - array of $1/RXMID$
 SLOPE - slope of temperature profile
 SPGRAV - specific gravity of gas
 T - temperature array ($^{\circ}K$)
 T0 - initial ground level temperature ($^{\circ}K$)
 TI - change in temperature array
 TADB - adiabatic temperature profile ($^{\circ}K$)
 TAMB - perturbation in temperature profile from ground ($^{\circ}K$)
 TIME - time (sec)
 TVAP - initial temperature of gas ($^{\circ}K$)
 U - radial velocity (M/sec)
 V - vertical velocity (M/sec)
 W - vorticity array (1/sec)
 WI - change in vorticity array during time setp (1/sec)
 WAMB - initial vorticity array (1/sec)
 Y - array of heights to bottom of zone
 YRATIO - ratio of vertical zone growth

Appendix D
DISCO

Equations (34), (35), and (36) are solved by numerical integration with the integration stepping forward in terms of downwind distance x . These equations are updated and the new values are saved for use during the next time or calculational cycle. Equation (33) is then solved and new velocities are calculated from the gradient of the stream function. The distance interval, Δx , is selected to satisfy numerical stability criteria associated with the advection or horizontal diffusion terms of each equation.

Again, as in the axi-symmetric model, the advection terms are solved using the Crowley 2nd Order Scheme. The horizontal diffusion term is solved using the centered second difference scheme and the vertical diffusion is solved from an implicit scheme discussed below.

Implicit Scheme for Vertical Diffusion

The implicit method used requires that certain intermediate quantities be stored while looping upwards and then the ϕ quantity is updated looping downwards.

Let

$$(D-1) \quad \phi_j^{n+1} = E_j \phi_{j+1}^{n+1} + G_j$$

Since this method requires immediate updating of the ϕ quantity, this is solved last. The other terms in this expression are given by:

$$(D-2) \quad E_j = -A_j / (B_j + C_j G_{j-1})$$

$$(D-3) \quad G_j = (D_j - C_j G_{j-1}) / (B_j + C_j E_{j-1})$$

$$(D-4) \quad B_j = 1.0 - A_j - C_j$$

$$(D-5) \quad D_j = \phi_j$$

$$(D-6) \quad A_j = F_{j+1/2} / \Delta y^2$$

$$(D-7) \quad C_j = F_{j-1/2} / \Delta y^2$$

$$(D-8) \quad F_{j+1/2} = \Delta t K_{j+1/2}$$

Stream Function Calculation

Equation (33) for the stream function is solved by means of Fourier transforms resulting in a direct solution of the differential equation. A second order finite difference approximation to the Poisson equation $\Delta^2 \psi = \eta$ is obtained by replacing the second derivative operator by a centered second difference operator.

$$(D-9) \quad \frac{\delta_y^2 \psi_{ij}}{(\Delta y)^2} + \frac{\delta_z^2 \psi_{ij}}{(\Delta z)^2} = \eta_{ij} \quad \begin{array}{l} i = 1, 2, \dots, I \\ j = 2, \dots, J-1 \end{array}$$

where

$$\delta_y^2 \psi_{ij} = \psi_{i+1,j} - 2\psi_{ij} + \psi_{i-1,j}$$

and

$$\delta_z^2 \psi_{ij} = \psi_{i,j+1} - 2\psi_{ij} + \psi_{i,j-1}$$

Boundary conditions are imposed as follows:

At the bottom of the mesh,

$$\psi_{i,1} = \alpha_i, \quad i = 1, \dots, I.$$

At the top of the mesh,

$$\psi_{i,J} = \beta_i, \quad i = 1, 2, \dots, I.$$

The cyclic boundary conditions in the horizontal area,

$$\psi_{0,j} = \psi_{I,j} \quad \text{and} \quad \psi_{1,j} = \psi_{I+1,j}, \quad j = 2, \dots, J-1.$$

We introduce an orthonormal base set of functions having cyclic properties on the index i :

$$w_{ik} = \sqrt{2/I} \cos \frac{2\pi ki}{I},$$

$$w_{i,I-k} = \sqrt{2/I} \sin \frac{2\pi ki}{I},$$

$$i = 1, 2, \dots, I$$

where I is even

$$w_{i,I} = 1/\sqrt{I}$$

$$k = 1, 2, \dots, \frac{I}{2} - 1.$$

These are the finite Fourier functions, which have the properties,

$$(D-10) \quad \sum_{i=1}^I w_{ik} w_{il} = \delta_{kl}$$

and the analogous cyclic boundary conditions are valid in the horizontal. They also have the property that they are eigenfunctions of the central second difference operator

$$\delta_y^2 w_{ik} = \lambda_k^2 w_{ik}$$

where $\lambda_k = 2 \sin \pi k/I$. These functions are complete functions on the interval $i = 1, 2, \dots, I$. Consequently, an arbitrary function f_i on this space can be represented

$$(D-11) \quad f_i = \sum_{k=1}^I a_k w_{ik}$$

where

$$a_k = \sum_{i=1}^I f_i w_{ik}$$

We are now ready to consider equation (D-9) from the point of view of Fourier transformation. The vorticity and stream function are represented as Fourier series as follows:

$$(D-12) \quad \eta_{ij} = \sum_{k=1}^I b_{kj} w_{ik} \quad , \quad \text{where } b_{kj} = \sum_{i=1}^I \eta_{ij} w_{ik}$$

and

$$(D-13) \quad \psi_{ij} = \sum_{k=1}^I a_{kj} w_{ik} \quad , \quad \text{where } a_{kj} = \sum_{i=1}^I \psi_{ij} w_{ik}$$

(1) The vorticity and the top and bottom boundary values of the stream function are subjected to Fourier transformation to obtain

$$b_{j\ell} = \sum_{i=1}^I \eta_{ij} w_{i\ell}$$

$$a_{1,\ell} = \sum_{i=1}^I a_i w_{i\ell} \quad \text{and}$$

$$a_{J,\ell} = \sum_{i=1}^I \beta_i w_{i\ell}$$

(2) The Fourier components of the stream function are obtained by solving the tridiagonal system of equations, equation (D-15) for $a_{j\ell}$.

(3) The stream function itself is obtained by Fourier synthesis

$$\psi_{ij} = \sum_{\ell=1}^I a_{j\ell} w_{i\ell}$$

The quantity I must be even. In order to take maximum advantage of the efficiency of the Fast Fourier Transform, the quantity I should also be a power of 2.

Substituting into equation (D-9) we obtain:

$$(D-14) \quad \sum_{k=1}^I w_{ik} - \frac{\lambda_k^2}{(\Delta y)^2} + \frac{\delta_a^2}{(\Delta z)^2} a_{ik} - b_{jk} = 0$$

Multiplying by $w_{i\ell}$ and summing over i gives

$$(D-15) \quad - \frac{\lambda_\ell^2}{(\Delta y)^2} + \frac{\delta_z^2}{(\Delta z)^2} a_{j\ell} = b_{j\ell}$$

$$j = 2, \dots, J-1$$

$$\ell = 1, 2, \dots, I$$

The values of $a_{1,\ell}$ and $a_{J,\ell}$ are obtained from the boundary values

$$a_{1,\ell} = \sum_{i=1}^I a_i w_{i\ell} \quad \text{and}$$

$$a_{J,\ell} = \sum_{i=1}^I \beta_i w_{i\ell}$$

In equation (D-15) the value of the wave number, ℓ , appears only parametrically. For each value of ℓ there is a tridiagonal equation having fixed values at the end points of the j -interval.

Summarizing the procedure for obtaining the direct solution of the Poisson equation, equation (D-9), by Fourier transform:

Program DISCO

The DISCO model is a two-dimensional hydrodynamics atmospheric dispersion code that ignores all interactions in the downwind direction. The model solves the conservation equations for energy, mass, and momentum as discussed in Section 2.

This model calculates the movement of a cloud in three dimensions by marching a slice of air downwind from the source. This two-dimensional plane is perpendicular to the wind direction and is advected at the ambient wind velocity.

There are a total of 20 subroutines and a main program within the DISCO model. The organization of all subroutines are shown in Figure D-1. Appropriate comment cards have been inserted throughout the code in order to provide an easily understandable program.

The DISCO main program is the driving routine that contains the primary loop in the program. The first subroutine called is INPUT1 which initializes several variables. The input parameters are obtained from DLINK and are passed through the common ZZBILL. Then the routine SETUP is called. This is a subroutine to DISCO and is not the same as the interactive SETUP program. SETUP initializes the coefficients to be used by the Fast Fourier Transfer routine.

The main loop of the program is entered next. First the Poisson equation is solved and the velocities in the plane are calculated. Then the eddy-diffusivities are computed based on the local stability and velocities. A time step is calculated for the computational cycle based on numerical stability criteria. Then the concentration, temperature, and vorticity arrays are updated by transporting the values with the local velocities and diffusing the values with the calculated diffusivities.

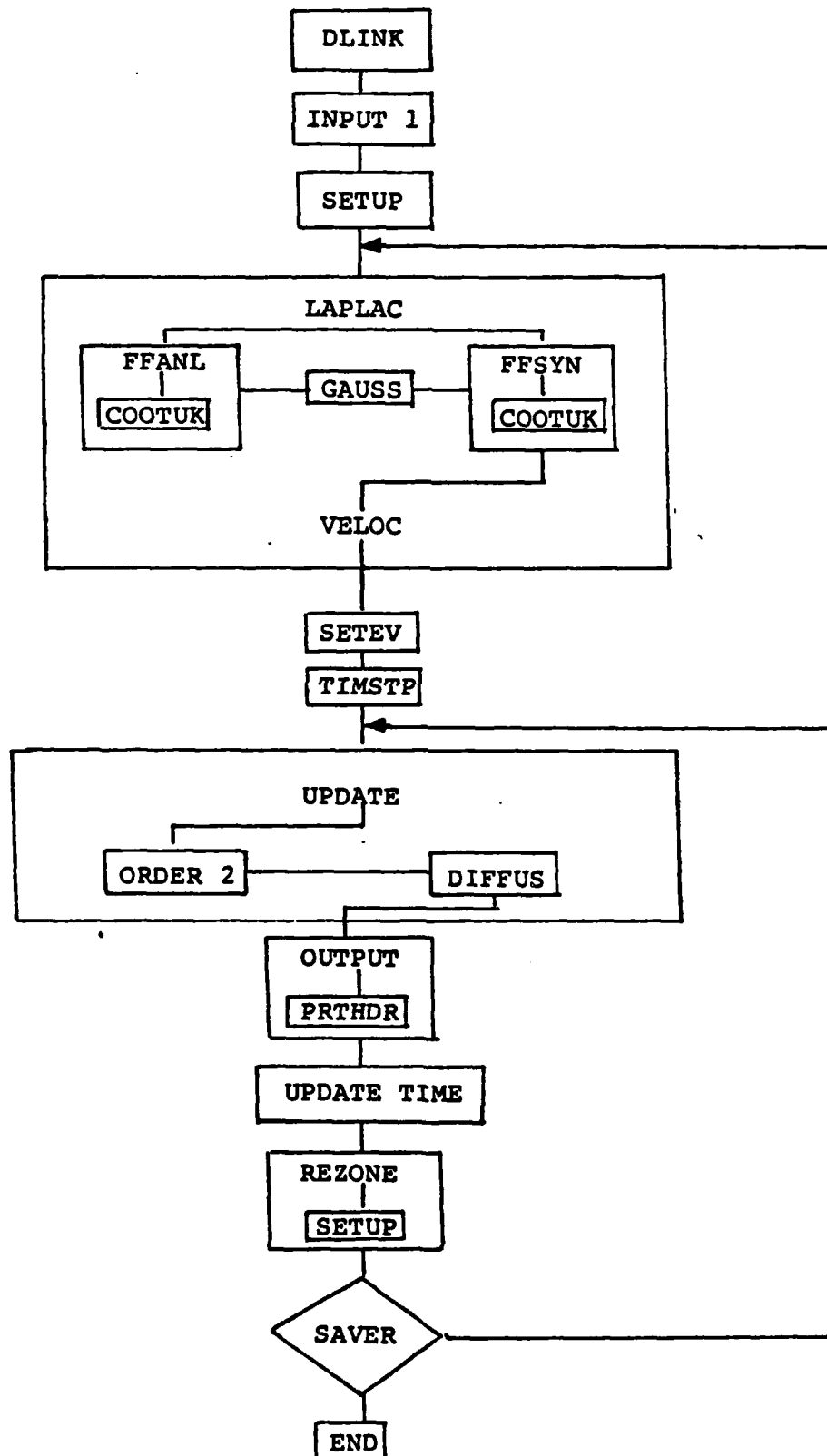


Figure D-1 Flowchart DISCO Dispersion Model

The output routine is entered and the cloud width to several concentrations are printed. The time (actually distance) is updated and the grid is checked to make sure the concentration of the pollutants is negligible at the boundaries. If the concentration is significant, the grid will be rezoned in either the horizontal or vertical direction or both.

The final routine SAVER checks for completion of the run. Also if the changes in the velocities are small, SAVER skips the calculation of velocities, diffusivities, and the time step.

Subroutines of DISCO

Subroutine INPUT1

INPUT1 initializes all of the variables and indices to be used for the problem. The input is obtained from DLINK through common ZZBILL. Also the grid dimensions and ambient profiles of pressure and temperature are generated. (see Figure D-2)

Subroutine SETUP

This routine sets up coefficients for the Fast Fourier Transfer routines. See Appendix D for details. All FFT routines are available in the literature and are not described in detail here.

Subroutine LAPLAC

This routine controls the solution of the Poisson's equation. See Appendix D.

Subroutine FFANL

Fast Fourier Analyzer. See Appendix D.

Subroutine GAUSS

Gauss Elimination in the vertical. See Appendix D.

SUBROUTINE INPUT 1

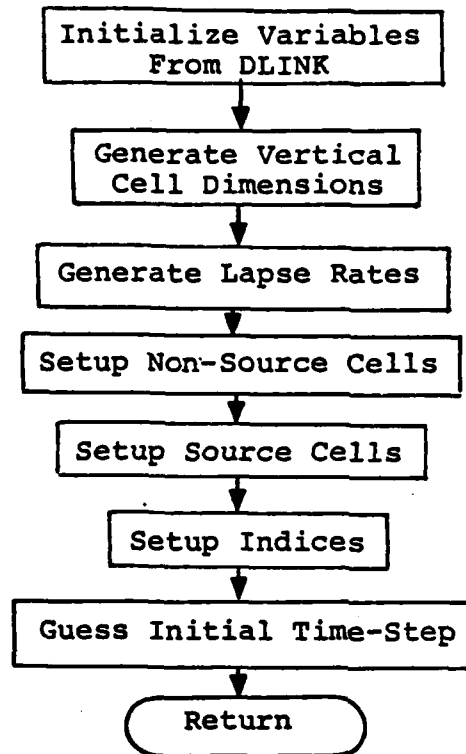


Figure D-2

Subroutine FFSYN

Fast Fourier Synthesizer. See Appendix D.

Subroutine XYPOIS

FFT routine used to call FFANL, GAUSS, and FFSYN.

Subroutine COOTUK

Cooley-Tukey Fast Fourier Transform Routine

Subroutine VELOC

VELOC calculates the velocity field based on the stream function psi. See Appendix D.

Subroutine SETEV

SETEV calculates the local eddy-diffusivities based on atmospheric stability and wind velocities. The data used is empirical from Smith and Howard. (see Figure D-3)

Subroutine TIMSTP

The routine TIMSTP calculates the internal time step based on numerical stability criteria. Actually, time is a distance in the computer code. (see Figure D-4)

Subroutine UPDATE

This routine calculates the changes in the scalar variables due to advection, diffusion, and heat transfer effects. Then this routine updates the old values of temperature, concentration and vorticity to find the new values at this downwind distance. (see Figure D-5)

Subroutine ORDER2

ORDER2 calculates the changes in the temperature concentration and vorticity arrays due to advection. These advection terms are solved utilizing a Crowley second order scheme. (see Figure D-6)

Subroutine SETEV

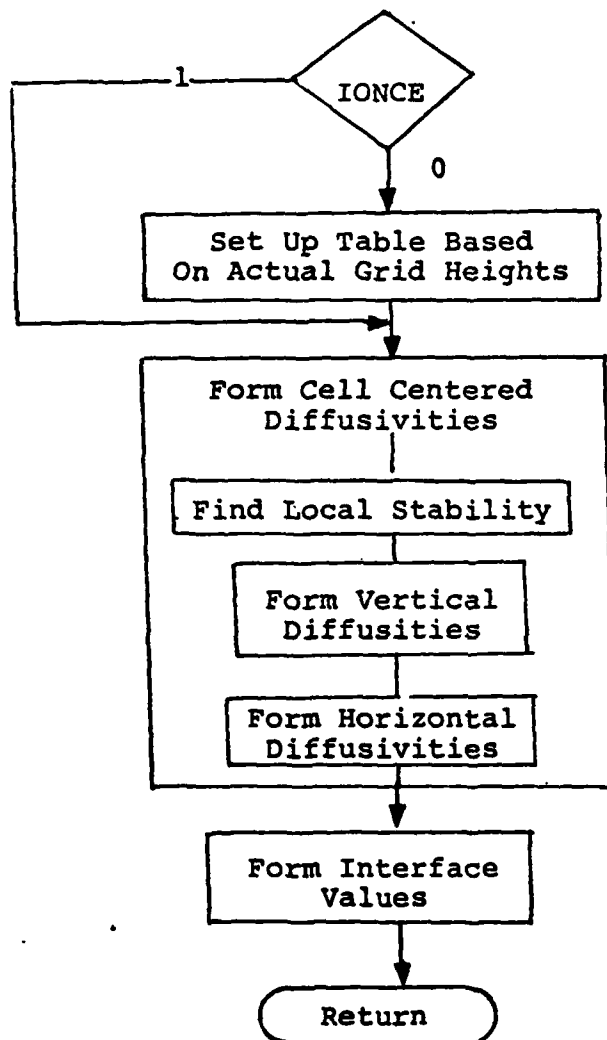


Figure D-3

SUBROUTINE TIMSTP

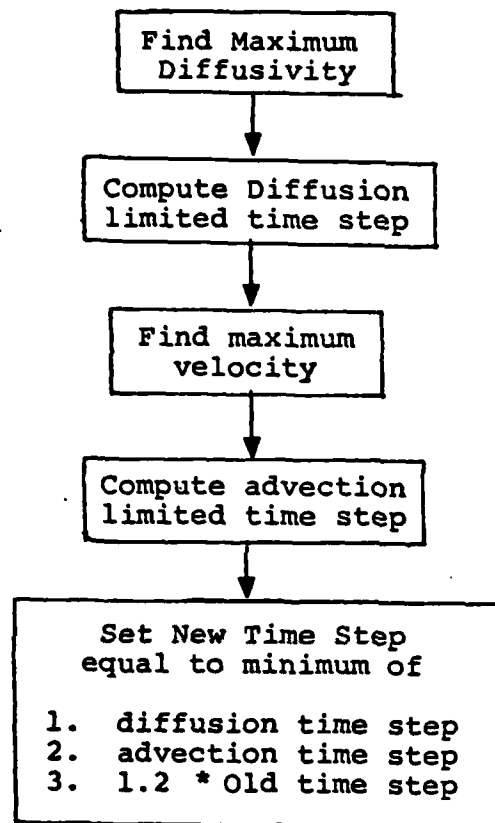


Figure D-4

SUBROUTINE UPDATE

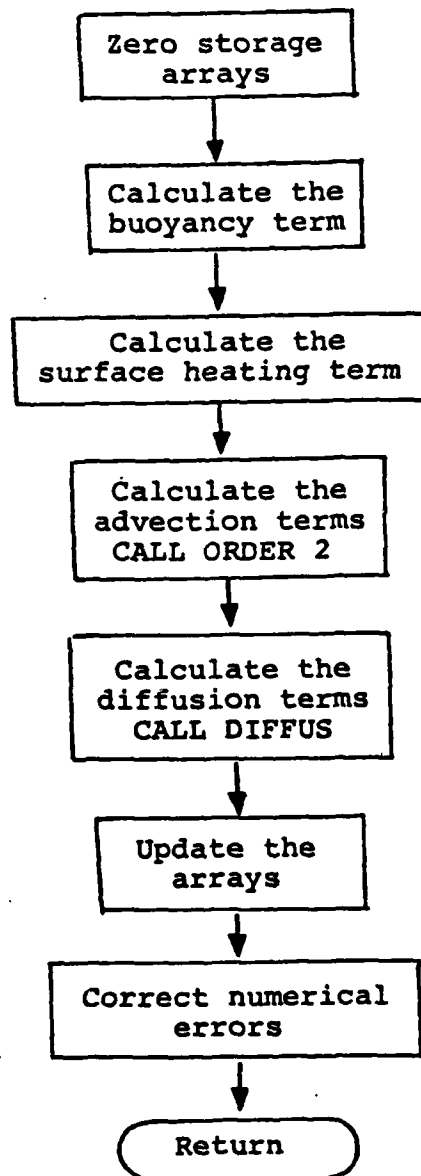


Figure D-5

SUBROUTINE ORDER 2

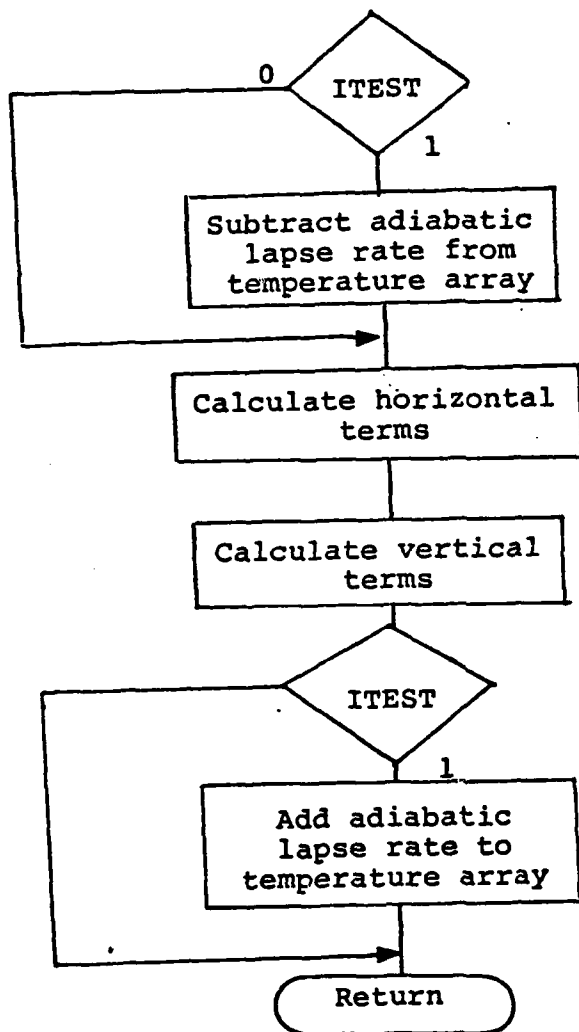


Figure D-6

Subroutine DIFFUS

DIFFUS calculates the diffusion terms using the eddy viscosities computed in SETEV. The horizontal terms are calculated using a standard second order centered difference scheme. The vertical terms are solved using an implicit method (see Figure D-7).

Subroutine OUTPUT

OUTPUT prints out the output of cloud width at a downwind distance. The width is found to the lower flammable limit, the stoichiometric limit, and to two toxicity limits of H_2S if required. Also the cloud height and the maximum concentration at each downwind distance are printed.

Subroutine REZONE

If a significant concentration of pollutant nears the edge of computational grid, the grid is rezoned to contain the entire problem within the grid. REZONE can change the grid scale in either vertical or horizontal direction or both. (see Figure D-8)

Subroutine SAVER

SAVER is the routine that determines if the problem is completed. This involves testing on whether the maximum concentration is less than the lower flammable limit. If H_2S is considered in the problem, then the maximum concentration is also compared to the 100ppm limit of H_2S . In addition, for situations where the velocity field is not changing, the SAVER routine skips LAPLAC, SETEV, and TIMSTP. (see Figure D-9)

Subroutine GETMAX

GETMAX finds the maximum value of the incoming array.

Subroutine GETMIN

GETMIN finds the minimum value of the incoming array

SUBROUTINE DIFFUS

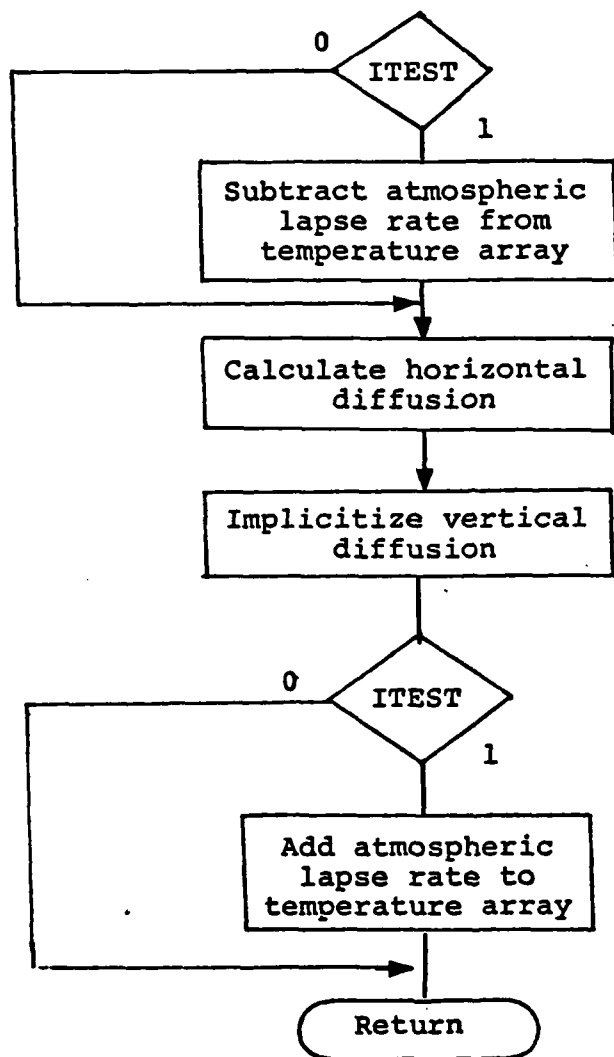


Figure D-7

SUBROUTINE REZONE

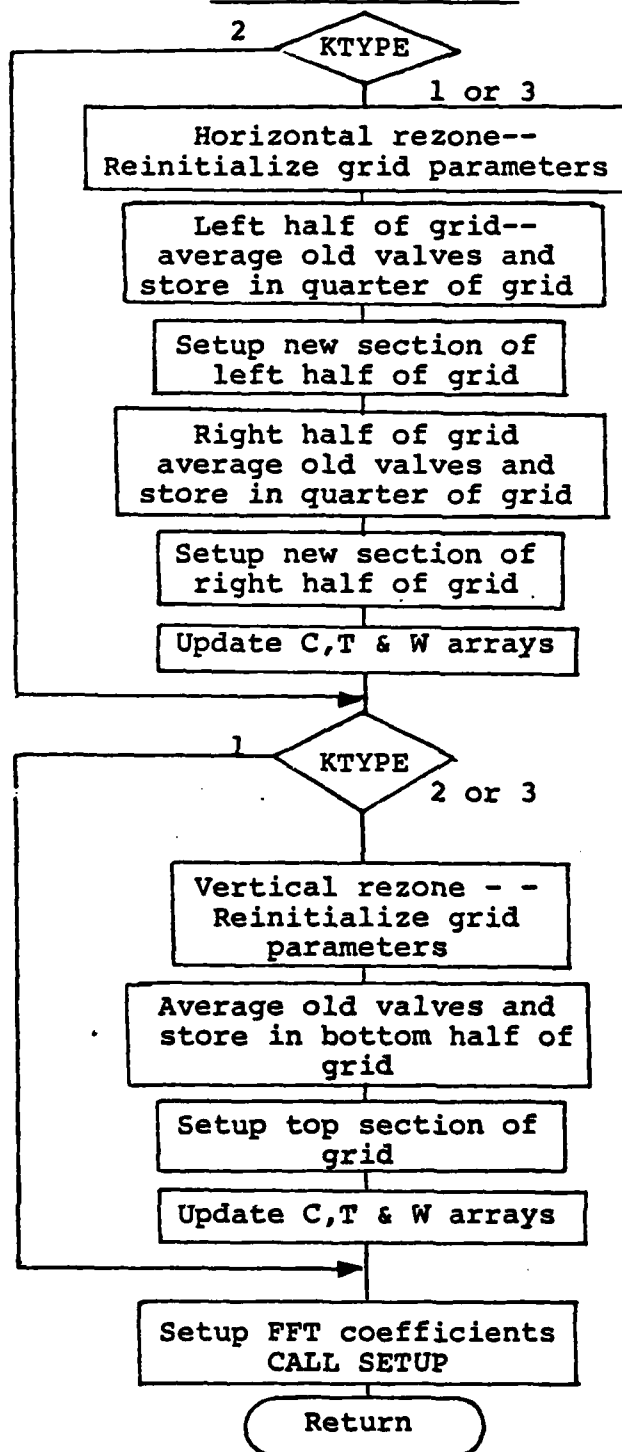


Figure D-8

SUBROUTINE SAVER

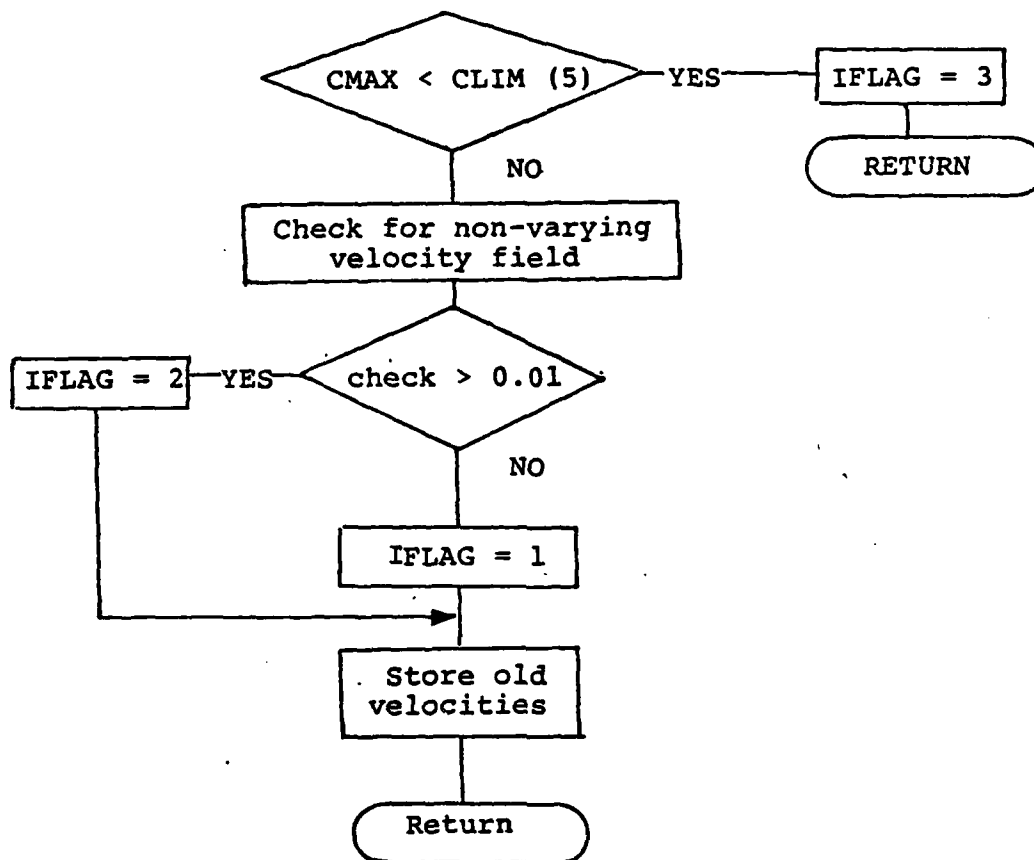


Figure D-9

MAIN Program Variables for DISCO Model

C - pollutant array (volume concentration)
C1 - stores one cycle changes in pollutant array
CINIT - initial pollutant concentration
CLIM - array containing flammable, toxicity and stoichiometric limits
CMAX - maximum pollutant concentration for this cycle
CPMETH - heat capacity of pollutant (c/gk°)
DIFDAT - empirical diffusion coefficients
DIFNOW - interpolated diffusion coefficients for current grid
DT - distance step for this cycle (meters)
DX - grid spacing in the horizontal direction (meters)
DY - grid spacing in the vertical direction-variable (meters)
DYCUM - cumulative heights (meters)
EVX - horizontal eddy diffusivity
EVY - vertical eddy diffusivity
HEATTC - heat transfer coefficient (J/kg°c)
IONCE - flag for SETEV if grid rezoned
MTEMP - adiabatic lapse rate (°c/m)
NX - grid zones in x direction
NX2 - NX divided by two
NXM1 - NX minus one
NXM2 - NX minus two
NXP1 - NX plus one
NY - grid zones in vertical direction
NYM1 - NY minus one
NYM2 - NY minus two
NYP1 - NY plus one
P - stream function array
PRMETH - pressure divided by gas constant for pollutant
R2DX - one half divided by DX
RDX - one divided by DX
RDX2 - one divided by DX squared

RR - coefficients used in FFT
 RTEMP - atmospheric lapse rate
 S1 - coefficient used in FFT
 SL - coefficient used in FFT
 SPGRAV - specific gravity of pollutant
 T - temperature array (°C)
 TI - stores one cycle changes in temperature array
 TAMB - ambient temperatures (°C)
 TIME - distance downwind (meters)
 TKELV - temperature Kelvin (273.16°)
 TLNG - initial temperature of pollutant (°K)
 TSURF - surface temperature (°C)
 TT - coefficient used in FFT
 U - horizontal velocity array (m/s)
 UI - stores old values of u velocity
 UFIX - initial wind velocity array (m/s)
 UU - coefficient used in FFT
 V - vertical velocity array (m/s)
 VV - coefficient used in FFT
 W - vorticity array
 W1 - stores one cycle changes in vorticity array
 WTOI - gravitational constant multiplied by TKELV
 Y - heights at center of each vertical zone (m)
 YBOTM - height of bottom vertical zone (m)
 YRATIO - ratio of heights between each vertical zone

APPENDIX E

Physical Properties

Calculation of Droplet Size Distribution

An analysis of the JP4 fuel venting from Aircraft inflight (E1) indicates that the expected droplet size would range from 0.5 micron to 2100 microns. The larger number is the maximum stable drop size for a free falling drop in the atmosphere whereas the small drop is estimated to be formed from the shearing between the liquid stream and the air velocity caused by the aircraft forward speed.

The maximum velocity expected from a fuel line break would be approximately 30 m/sec which is significantly less than aircraft speed. This would suggest that the sprayed droplets would tend to be somewhat larger than would be expected from the fuel dumping from an inflight aircraft. In actual situations, a single droplet size would not be produced but a distribution could be expected. In addition, a significant time would be required for oversized droplets to become unstable and "break-up" into smaller droplets. The fuel dump experiments (E1) resulted in a measured droplet distribution with the median drop diameter of several 100 microns. For the problem of spray from a failed pressurized line, the sizes are expected to be larger and result in droplet sizes of several thousands microns. For our nominal calculations a 3000 micron droplet diameter was used.

Calculation of Drag Coefficient for Spherical Droplets

Figure E-1 presents data for the drag coefficient C_D of a sphere moving through air as a function of the Reynolds number. For this study, an approximate Reynolds number may be calculated as:

$$Rey_n = \frac{\rho_a VD}{\mu}$$

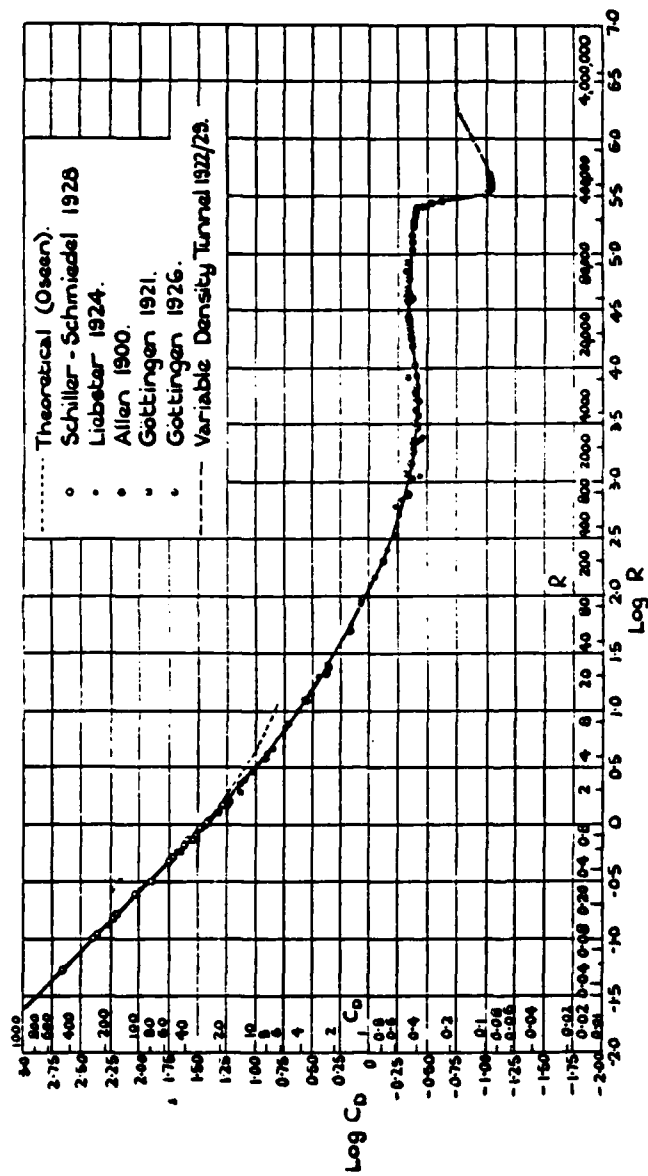


Figure E-1
Drag Coefficient as a Function of Reynolds
Number from (E2)

where

μ = air viscosity

D = droplet diameter

ρ_a = air density

The velocity of the droplet may be calculated using Bernoulli's equation as indicated below:

$$\frac{\Delta P}{\rho} = \frac{1}{2} \frac{V^2}{g}$$

For a fueling operation, the fuel line pressure is approximately 50 psig. The velocity associated with a droplet emitted from a hole in the line is calculated to be 96 ft/sec. (≈ 29 m/sec). Figure E-2 shows the drag coefficient, C_D , as a function of droplet diameter and wind speed assuming standard atmospheric conditions. Reynolds numbers vary from approximately 5 ($U = 1$ m/sec, $D = 500$ microns) to 9500 ($U = 50$ m/sec, $D = 2000$ microns).

For the purposes of the phase I study, the C_D was assumed constant at a value of approximately 0.4 ie, the approximate value for droplet diameters greater than 500 at a velocity of 30 m/sec. During phase II, calculations will be performed to determine if further definition of this variable is required.

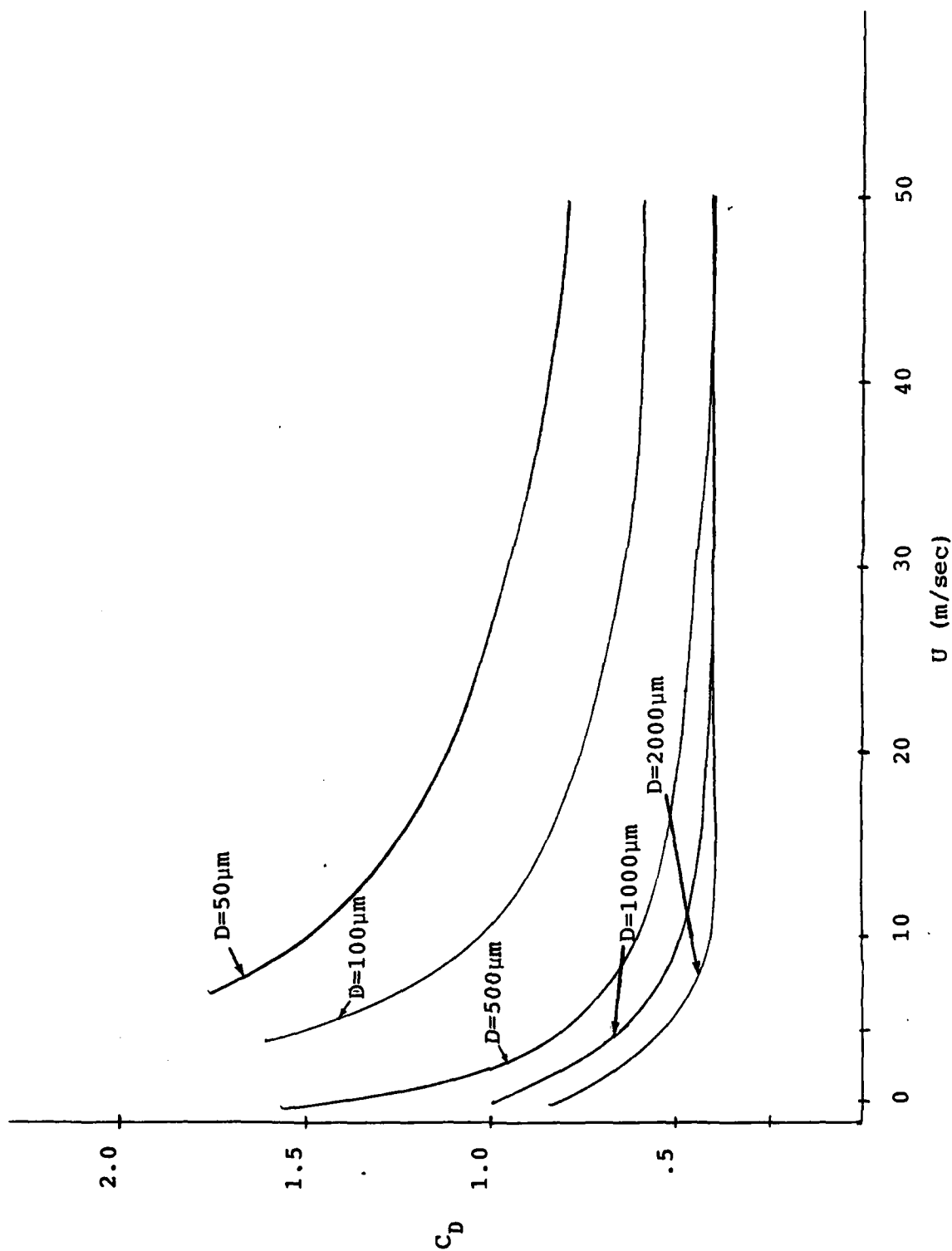


FIGURE E-2
 DRAG COEFFICIENT VS. WIND SPEED AS A
 FUNCTION OF DROPLET DIAMETER

Calculation of Turbulent Eddy Diffusivities

For the model, an ambient turbulence model according to Hanna (E3) and correlated by Smith and Howard (E4) was adopted. Hanna has suggested a form for the equation expressing the local diffusivity which can be expressed in any of the following equivalent forms,

$$(E-1) \quad K_a = 0.09 \sigma_w k_m^{-1}$$

$$(E-2) \quad K_a = 0.06 \epsilon^{1/3} k_m^{-1}$$

$$(E-3) \quad K_a = 0.35 \sigma_w^4 \epsilon^{-1}$$

where σ_w is the standard deviation of the vertical turbulence, ϵ is the rate of dissipation of turbulent energy, and k_m is the wave number where the vertical turbulent energy spectrum is a maximum. Hanna evaluated the constants given in these equations through the use of observational data. The ambient turbulence eddy diffusivity K_a was evaluated alternately by equations with arbitrary constants and an equation relating the atmospheric momentum flux to the mean velocity shear. The relation between the two yielded the values of the constants given.

Numerous measurements of σ_w have also been made under a variety of conditions. Alternately, K_a was related to a turbulence scale length (l) by Taylor, Warner and Bacon (E5):

$$(E-4) \quad l = \frac{0.2}{k_m}$$

Because of the ready availability of observational data, this study uses a solution technique where K_a is calculated as

$$(E-5) \quad K_a = 0.45 \sigma_w l = 0.45 u \sigma_e l$$

since σ_w is equal to $u \sigma_e$ where u is the local velocity and σ_e is equivalent to a measurement of wind vane fluctuations in radians. The values of σ_e and l are functions of height and atmospheric stabilities and the values used in this study are summarized in Tables E-1 and E-2.

AD-A164 045

DEVELOPMENT OF A FUEL SPILL/VAPOR MIGRATION MODELING
SYSTEM(U) TRACER TECHNOLOGIES ESCONDIDO CA*
W G ENGLAND ET AL. DEC 85 AFMIL-TR-85-2089

2/2

UNCLASSIFIED

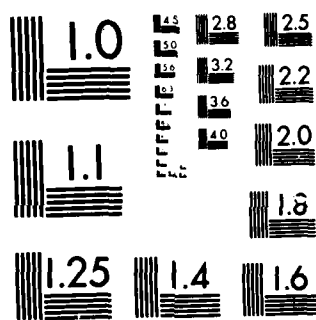
F33615-83-C-2472

F/G 21/4

NL

END

FILED
100
DTIC



MICROCOPY RESOLUTION TEST CHART
NATIONAL BUREAU OF STANDARDS-1963-A

TABLE E-1

Variations in σ_e

Stability Class	σ_e (0-10m)	σ_e (30 m and 100 m)
A	0.200 (radians)	0.262 (radians)
B	0.185	0.237
C	0.157	0.184
D	0.117	0.119
E	0.061	0.056
F	0.028	0.023
G	0.012	0.009

TABLE E-2

Turbulence Scale Lengths (z)

z (m)	A	B	C	D	E	F	G
0-10	18	15	12	10	8	7	6
20	30	25	21	18	16	14	12
30	41	34	29	25	22	20	17
50	62	52	44	39	35	31	27
75	84	71	60	52	48	43	37
100	105	85	74	64	60	54	46

The horizontal diffusivity differs from the vertical diffusivity by a factor which also depends on the atmospheric stability. In a stable atmosphere the horizontal

diffusivity is relatively enhanced over the vertical, while in an unstable atmosphere the opposite is the case, although to a lesser degree. In Table E-3 we give the ratio of horizontal to vertical diffusivity as a function of Pasquill category stability classes according to Lantz (E6).

Based on field data gathered over four years by SAI (E7), values of $K_{a,x}/K_{a,z}$ of 1.0, 10.0, and 25.0 have been used in the calculations presented for stability classes D, E, and F. The values are conservative compared to those of Lantz.

TABLE E-3

Ratio of Horizontal and Vertical
Diffusivities Versus Stability Class

Ratio		Stability					
		A	B	C	D	E	F
K_x/K_z	Lantz	0.1	0.5	1.5	6	19	65
	SAI	1.0	1.0	1.0	1.0	10	15

SOURCE RATE SPECIFICATION FOR DISPERSION MODELS

The axi-symmetric dispersion model requires a source rate be specified that is both time and position dependent. For the pipe rupture the source codes provide the time dependent release rate and the release is positioned at

the break in the first grid cell. The tank failure pool spread models give both the pool position and vaporization rate as functions of time for direct input into the dispersion model.

The quasi-three dimensional dispersion model requires a steady state source rate be specified. The source rate data provided by the source modes1 is, therefore, converted into an equivalent steady source using an averaging scheme consistent with the fundamental assumptions involved in the quasi-three dimensional dispersion model. The grid is positioned at the break for pipeline failures and at the center of the pool in the liquid spills.

Source Model Parameters

Cicccone and Graves (E8), in a study of fuel tank leak classification, measured the surface area of spill as a function of the spill size. An analysis was made of the data presented in the report and it was concluded that the thickness of the liquid pool would be approximately 0.0005 meters (.5mm). This number was used to estimate the final pool spill size in the model.

The other information obtained from the literature was the vaporization rate for a droplet. Mackay and Matsugu (E9) provide the basic theory for liquid spills of hydrocarbons on land. However, one of the unknowns in that theory is the average vapor partial pressure above the liquid pool. The maximum evaporation rate can be determined by assuming that the vapor partial pressure in the atmosphere is zero. Dawbarn, Nutt and Pender (E10) have made measurements on the vaporization rate of small droplets in a wind tunnel. This information on the droplet vaporization rate was compared with the theory and it was determined that a nominal partial pressure of .755 times the vapor pressure provided the best fit to the data. Figure E-3 provides a comparison of the measured data and the fit. This fit or $P_{\infty} = 0$ was utilized for calculations presented in this report giving a range of hazard distances as a function of this parameter.

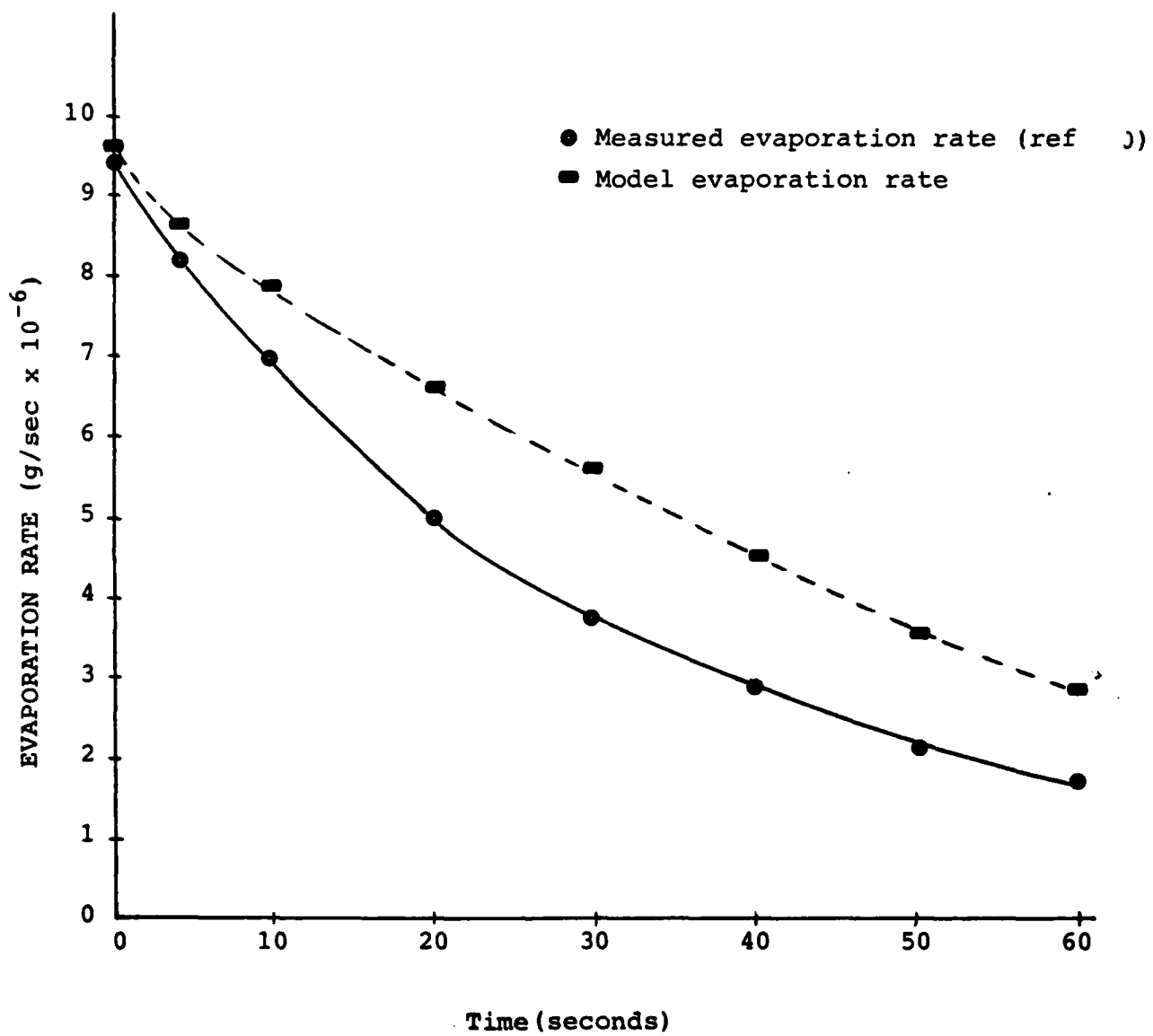


Figure E-3
Droplet Evaporation Rate for a 500 Micron Radius
Droplet as a Function of Time (U=10 mph, T=20°C)

REFERENCES

- E1. Good, E., C.A. Forsberg, and Patricia M. Bench, "Breakup Characteristics of JP-4 Vented from KC-135 Aircraft", Air Force Geophysics Lab, AFGL-TR-78-0190, AD-B035425, August 1978.
- E2. Goldstein, S. "Modern Developments in Fluid Dynamics", Dover Publications, New York, 1965.
- E3. Hanna, S., "A Method of Estimating Vertical Eddy Transport in the Planetary Boundary Layer Using Characteristics of the Vertical Velocity Spectrum." J. Atmos. Sci., 25, 1026-1033, 1968.
- E4. Smith, T.B. and Howard, S.M.; Methodology for Treating Diffusivity, Final Report submitted to Systems, Science and Software by Meteorology Research, Inc., September 6, 1972.
- E5. Taylor, R.J., J. Warner, and N.E. Bacon, "Scale Length in Atmospheric Turbulence as Measured From an Aircraft", CSIRO Division of Radiophysics, Australia, Quart.J. Roy. Meteor. Soc., 96, 750-755, 1970.
- E6. Lantz, R.B., Coats, K.H. and Kloepper, C.V. "A Three-Dimensional Numerical Model for Calculating the Spread and Dilution of Air Pollutants." Presented at the Air Pollution Turbulence and Diffusion Symposium, December 7-10, 1972.
- E7. "LNG Terminal Risk Assessment Study for Oxnard, California", Science Applications, Inc. Report to Western LNG Terminal Company, December, 1975.
- E8. Ciccone, V.J. and A.P. Graves, "A Study to Evaluate the Intensity of Alternative Methods for Neutralization of DOD Aircraft Fuel Spills." DOD Aircraft Ground Fire Suppression and Rescue Office, AD-A025937, Feb. 1976.
- E9. Mackay, D. and R.S. Matsugu, "Evaporation Rates of Liquid Hydrocarbon Spills on Land and Water", The Canadian Journal of Chemical Engineering, Vol. 51, August, 1973, pp 434-439.
- E10. Dawbarn, R., K.W. Nutt, and C.W. Pender, "A Study of the Jettisoning of JP-4 Fuel in the Atmosphere", Arnold Engineering Development Center, AEDC-TR-75-49, AD-A017555, Nov. 1975.

APPENDIX F

Sample Model Results

Liquid Spill Model Results

Spill Volume (cu m) = .1514
 Wind Speed (m/sec) = 2.23
 Air Temperature (c) = 20.00
 Fuel Temperature (c) = 20.00
 Pool Radius (m) = 9.82

TIME SEC	TEMP C	VAPOR RATE KG/SEC	POOL MASS KG
.0000E+01	.2932E+03	.0000E+01	.1151E+03
.5000E+01	.2921E+03	.2409E+00	.1138E+03
.1000E+02	.2919E+03	.2381E+00	.1127E+03
.1500E+02	.2918E+03	.2376E+00	.1115E+03
.2000E+02	.2918E+03	.2375E+00	.1103E+03
.2500E+02	.2918E+03	.2375E+00	.1091E+03
.3000E+02	.2918E+03	.2375E+00	.1079E+03
.3500E+02	.2918E+03	.2375E+00	.1067E+03
.4000E+02	.2918E+03	.2375E+00	.1055E+03
.4500E+02	.2918E+03	.2375E+00	.1043E+03
.5000E+02	.2918E+03	.2375E+00	.1032E+03
.5500E+02	.2918E+03	.2375E+00	.1020E+03
.6000E+02	.2918E+03	.2375E+00	.1008E+03
.6500E+02	.2918E+03	.2375E+00	.9959E+02
.7000E+02	.2918E+03	.2375E+00	.9841E+02
.7500E+02	.2918E+03	.2375E+00	.9722E+02
.8000E+02	.2918E+03	.2375E+00	.9603E+02
.8500E+02	.2918E+03	.2375E+00	.9484E+02
.9000E+02	.2918E+03	.2375E+00	.9366E+02
.9500E+02	.2918E+03	.2375E+00	.9247E+02
.1000E+03	.2918E+03	.2375E+00	.9128E+02
.1050E+03	.2918E+03	.2375E+00	.9010E+02
.1100E+03	.2918E+03	.2375E+00	.8891E+02
.1150E+03	.2918E+03	.2375E+00	.8772E+02
.1200E+03	.2918E+03	.2375E+00	.8653E+02
.1250E+03	.2918E+03	.2375E+00	.8535E+02
.1300E+03	.2918E+03	.2375E+00	.8416E+02
.1350E+03	.2918E+03	.2375E+00	.8297E+02
.1400E+03	.2918E+03	.2375E+00	.8178E+02
.1450E+03	.2918E+03	.2375E+00	.8060E+02
.1500E+03	.2918E+03	.2375E+00	.7941E+02
.1550E+03	.2918E+03	.2375E+00	.7822E+02
.1600E+03	.2918E+03	.2375E+00	.7703E+02
.1650E+03	.2918E+03	.2375E+00	.7585E+02
.1700E+03	.2918E+03	.2375E+00	.7466E+02
.1750E+03	.2918E+03	.2375E+00	.7347E+02
.1800E+03	.2918E+03	.2375E+00	.7229E+02
.1850E+03	.2918E+03	.2375E+00	.7110E+02
.1900E+03	.2918E+03	.2375E+00	.6991E+02
.1950E+03	.2918E+03	.2375E+00	.6872E+02
.2000E+03	.2918E+03	.2375E+00	.6754E+02
.2050E+03	.2918E+03	.2375E+00	.6635E+02
.2100E+03	.2918E+03	.2375E+00	.6516E+02
.2150E+03	.2918E+03	.2375E+00	.6397E+02
.2200E+03	.2918E+03	.2375E+00	.6279E+02
.2250E+03	.2918E+03	.2375E+00	.6160E+02

Droplet Model Results

DROPLET MODEL

DROP RADIUS = .1500E+04

RELEASE ANGLE = 45.000

RELEASE VELOCITY = .3000E+02

AIR TEMPERATURE = 20.0

FUEL TEMPERATURE = 20.0

X	Y	TIME	U	V	MASS	RDOT
.9044E+00	.8833E+00	.5000E-01	.1809E+02	.1767E+02	.1074E-04	.3996E-06
.1693E+01	.1634E+01	.1000E+00	.1577E+02	.1501E+02	.1072E-04	.3525E-06
.2392E+01	.2281E+01	.1500E+00	.1398E+02	.1294E+02	.1071E-04	.3153E-06
.3019E+01	.2844E+01	.2000E+00	.1255E+02	.1126E+02	.1069E-04	.2851E-06
.3589E+01	.3338E+01	.2500E+00	.1139E+02	.9868E+01	.1068E-04	.2599E-06
.4110E+01	.3772E+01	.3000E+00	.1042E+02	.8681E+01	.1066E-04	.2385E-06
.4590E+01	.4154E+01	.3500E+00	.9609E+01	.7650E+01	.1065E-04	.2200E-06
.5036E+01	.4491E+01	.4000E+00	.8913E+01	.6739E+01	.1064E-04	.2038E-06
.5451E+01	.4787E+01	.4500E+00	.8311E+01	.5924E+01	.1063E-04	.1894E-06
.5841E+01	.5046E+01	.5000E+00	.7785E+01	.5183E+01	.1062E-04	.1765E-06
.6207E+01	.5272E+01	.5500E+00	.7321E+01	.4503E+01	.1061E-04	.1649E-06
.6552E+01	.5465E+01	.6000E+00	.6910E+01	.3870E+01	.1060E-04	.1545E-06
.6879E+01	.5629E+01	.6500E+00	.6542E+01	.3276E+01	.1060E-04	.1450E-06
.7190E+01	.5765E+01	.7000E+00	.6211E+01	.2714E+01	.1059E-04	.1364E-06
.7485E+01	.5873E+01	.7500E+00	.5912E+01	.2175E+01	.1058E-04	.1286E-06
.7768E+01	.5956E+01	.8000E+00	.5641E+01	.1655E+01	.1058E-04	.1217E-06
.8037E+01	.6014E+01	.8500E+00	.5393E+01	.1149E+01	.1057E-04	.1157E-06
.8296E+01	.6046E+01	.9000E+00	.5166E+01	.6525E+00	.1056E-04	.1105E-06
.8543E+01	.6054E+01	.9500E+00	.4958E+01	.1612E+00	.1056E-04	.1063E-06
.8782E+01	.6038E+01	.1000E+01	.4766E+01	-.3289E+00	.1055E-04	.1031E-06
.9011E+01	.5997E+01	.1050E+01	.4587E+01	-.8162E+00	.1055E-04	.1011E-06
.9232E+01	.5932E+01	.1100E+01	.4422E+01	-.1297E+01	.1054E-04	.1001E-06
.9446E+01	.5844E+01	.1150E+01	.4268E+01	-.1768E+01	.1054E-04	.1003E-06
.9652E+01	.5732E+01	.1200E+01	.4125E+01	-.2226E+01	.1053E-04	.1013E-06
.9851E+01	.5599E+01	.1250E+01	.3991E+01	-.2667E+01	.1053E-04	.1031E-06
.1004E+02	.5445E+01	.1300E+01	.3865E+01	-.3089E+01	.1052E-04	.1055E-06
.1023E+02	.5270E+01	.1350E+01	.3747E+01	-.3491E+01	.1052E-04	.1083E-06
.1041E+02	.5077E+01	.1400E+01	.3636E+01	-.3871E+01	.1051E-04	.1113E-06
.1059E+02	.4865E+01	.1450E+01	.3531E+01	-.4227E+01	.1051E-04	.1145E-06
.1076E+02	.4637E+01	.1500E+01	.3432E+01	-.4560E+01	.1050E-04	.1176E-06
.1093E+02	.4394E+01	.1550E+01	.3339E+01	-.4868E+01	.1049E-04	.1206E-06
.1109E+02	.4136E+01	.1600E+01	.3250E+01	-.5154E+01	.1049E-04	.1236E-06
.1125E+02	.3865E+01	.1650E+01	.3166E+01	-.5416E+01	.1048E-04	.1263E-06
.1140E+02	.3583E+01	.1700E+01	.3087E+01	-.5656E+01	.1048E-04	.1289E-06
.1155E+02	.3289E+01	.1750E+01	.3011E+01	-.5874E+01	.1047E-04	.1312E-06
.1170E+02	.2985E+01	.1800E+01	.2939E+01	-.6073E+01	.1046E-04	.1334E-06
.1185E+02	.2673E+01	.1850E+01	.2870E+01	-.6253E+01	.1046E-04	.1353E-06
.1199E+02	.2352E+01	.1900E+01	.2804E+01	-.6415E+01	.1045E-04	.1371E-06
.1212E+02	.2024E+01	.1950E+01	.2741E+01	-.6561E+01	.1044E-04	.1387E-06
.1226E+02	.1689E+01	.2000E+01	.2681E+01	-.6692E+01	.1044E-04	.1400E-06
.1239E+02	.1349E+01	.2050E+01	.2624E+01	-.6810E+01	.1043E-04	.1413E-06
.1252E+02	.1003E+01	.2100E+01	.2569E+01	-.6915E+01	.1042E-04	.1424E-06
.1264E+02	.6524E+00	.2150E+01	.2516E+01	-.7009E+01	.1041E-04	.1433E-06
.1277E+02	.2978E+00	.2200E+01	.2465E+01	-.7092E+01	.1041E-04	.1441E-06
.1289E+02	-.6056E-01	.2250E+01	.2416E+01	-.7166E+01	.1040E-04	.1449E-06

Dispersion Model Results

Dispersion Model Input Parameters

Wind Speed = 5.0 m/sec

Air Temperature = 293 °C

Source Rate = .38 kg/sec

Stability Class = F

Liquid Pool Radius = 9.8 m

DOWNWIND DISTANCE (METERS)	MAXIMUM CLOUD CONCENTRATION LIMIT (V/V)	CLOUD WIDTH LOWER FLAMMABLE MIXING RATIO (1.3%) (METERS)	CLOUD WIDTH STOICHIOMETRIC MIXING RATIO (4.0%) (METERS)	CLOUD HEIGHT STOICHIOMETRIC MIXING RATIO (4.0%) (METERS)
0. 00000E+00	0. 99947	19. 640	19. 640	0. 76321E-03
0. 12043E-01	0. 99939	19. 640	19. 640	0. 76321E-03
0. 26496E-01	0. 64141E-01	19. 640	19. 640	0. 86087E-02
0. 43838E-01	0. 45062E-01	19. 640	19. 640	0. 60182E-02
0. 64649E-01	0. 36094E-01	19. 640	0. 00000E+00	0. 00000E+00
0. 89623E-01	0. 30013E-01	19. 640	0. 00000E+00	0. 00000E+00
0. 11959	0. 25521E-01	19. 640	0. 00000E+00	0. 00000E+00
0. 15555	0. 22031E-01	19. 640	0. 00000E+00	0. 00000E+00
0. 19871	0. 19217E-01	19. 640	0. 00000E+00	0. 00000E+00
0. 25049	0. 16886E-01	19. 640	0. 00000E+00	0. 00000E+00
0. 31263	0. 16722E-01	19. 640	0. 00000E+00	0. 00000E+00
0. 31609	0. 16566E-01	19. 640	0. 00000E+00	0. 00000E+00
0. 32023	0. 16388E-01	19. 640	0. 00000E+00	0. 00000E+00
0. 32521	0. 16186E-01	15. 712	0. 00000E+00	0. 00000E+00
0. 33118	0. 15955E-01	15. 712	0. 00000E+00	0. 00000E+00
0. 33834	0. 15693E-01	15. 712	0. 00000E+00	0. 00000E+00
0. 34694	0. 15397E-01	15. 712	0. 00000E+00	0. 00000E+00
0. 35725	0. 15067E-01	15. 712	0. 00000E+00	0. 00000E+00
0. 36963	0. 14699E-01	15. 712	0. 00000E+00	0. 00000E+00
0. 38449	0. 14294E-01	15. 712	0. 00000E+00	0. 00000E+00
0. 40231	0. 13851E-01	15. 712	0. 00000E+00	0. 00000E+00
0. 42370	0. 13371E-01	15. 712	0. 00000E+00	0. 00000E+00
0. 44937	0. 12857E-01	0. 00000E+00	0. 00000E+00	0. 00000E+00

END

FILMED

386

DTIC